Chapter 13

Magnetic actuation of flexible and soft robotic systems for medical applications

Venkatasubramanian Kalpathy Venkiteswaran[a] and Sarthak Misra[a,b]
[a]*Surgical Robotics Laboratory, Department of Biomechanical Engineering, University of Twente, Enschede, The Netherlands,* [b]*Surgical Robotics Laboratory, Biomaterials and Biomedical Technology, University Medical Centre Groningen, University of Groningen, Groningen, The Netherlands*

1. Introduction

Robotic systems were initially developed to automate manual tasks typically performed by industrial workers, such as precisely positioning objects along assembly lines. The initial wave of robotic systems that reached a level of maturity suitable for commercial applications centered around articulated robotic arms. This development in industrial robotics also sparked interest in the medical field, where researchers explored the potential of employing articulated manipulators as substitutes for human clinicians in tasks such as tool positioning and tissue extraction during surgical procedures.

In medical procedures, the first robotic systems were employed in the realm of stereotactic surgery, particularly in minimally invasive procedures aimed at the central nervous system [1]. Thus, a neurosurgical procedure of image-guided needle biopsy of the brain became the first clinical application of robotics [2]. Following this initial success, articulated robots were proposed for autonomous tasks within other medical disciplines [3]. However, the widespread adoption of these devices has not been supported by compelling results to warrant their large-scale clinical deployment. The concept of autonomous operation presents inherent challenges, particularly concerning the legal responsibility for any failures of the device. Additionally, these robots have been encumbered by both technical complexities and economic constraints.

Contemporary perspectives on robotic technology in minimally invasive surgery (MIS) acknowledge the unique capabilities of human operators in planning and overseeing manual tasks. Instead of seeking to entirely supplant

Recent Progress in Medical Miniature Robots. https://doi.org/10.1016/B978-0-443-13385-5.00012-X

clinicians, modern robotic systems are conceived as advanced surgical instruments for collaborative use. Employed by clinicians in real-time through specialized interfaces, these systems aim to enhance human abilities on a smaller scale, facilitating a synergistic partnership between humans and machines in the surgical setting [4]. The most commercially successful system embodying this approach is certainly the da Vinci Surgical System (Intuitive Surgical, Sunnyvale, CA, USA). First used in 1997 in laparoscopic cholecystectomy in Belgium, it received Food and Drug Administration (FDA) approval in 2000. Since then, Da Vinci became the de facto standard tool for robotic endoscopic surgery [5].

The success of da Vinci in endoscopic applications motivated the intensification of surgical robotics research both in academia and industry. The general objective of this research was to explore and develop viable robotic technologies that enable a broader range of surgical procedures to be conducted using minimally invasive techniques. Particular emphasis was put on potential solutions for reducing the invasiveness of procedures performed in challenging locations, such as inside the brain or the heart. The need for miniaturization renders the use of articulated arms in such procedures near impossible, with associated risks of tissue damage they impose, due to their inherent rigidity [6]. Thus, the attention of the surgical robotics community has focused instead on various groups of manually operated flexible surgical instruments, such as needles, catheters, and endoscopes, which are used when minimally invasive access to a remote target is required.

From an engineering perspective, flexible surgical instruments are continuum devices. Their behavior differs significantly from the one of industrial robotic arms. Continuum devices (see Fig. 1) do not bend in discrete locations, but incorporate elastic elements, which *continuously* change shape in response to mechanical loads [7]. This property allows them to inherently respond to the environmental forces upon contact. The safety of that contact is determined by the degree of their compliance matching with the environment. Nevertheless, flexible instruments with compliance closely matching the one of soft tissues experience significant deformation in response to unpredictable external loads present within the surgery site [8]. This fact restricts their precision during manual operation. To remedy that, dedicated sensing and actuation means can be integrated into the structure of flexible surgical instruments to harness their continuum nature. The resulting systems—continuum robots—offer completely new opportunities for surgical procedures realized in a minimally invasive fashion [9].

Taking the concept of flexibility even further, soft robots have strong potential for use in medical applications, particularly MIS, since their shape-programmable soft bodies are more flexible than their rigid counterparts in enclosed and confined spaces [10,11]. Existing soft robots have been demonstrated to be maneuverable and controllable [12]. However, soft robots intended for MIS are required to be not only flexible, but also functional, biocompatible, and scalable to small sizes.

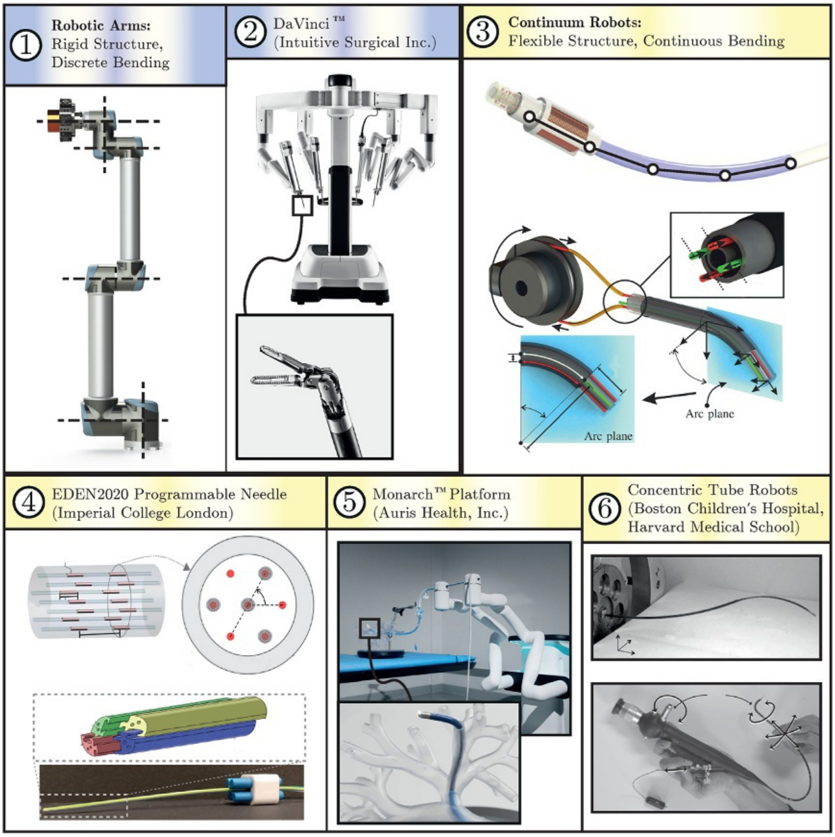

FIG. 1 The two main classes of robotic devices used in surgical procedures are rigid robotic arms (blue) and continuum robots (yellow). ① Rigid robotic arms with stiff links connected by discrete motorized joints. ② da Vinci Surgical System employing robotic manipulators for teleoperated endoscopic procedures. ③ Continuum robots use deformation of elastic elements within their entire structure to generate motion. In addition to catheters, other principal types of continuum robots used for surgical procedures involve: ④ flexible needles, ⑤ steerable endoscopes, among them the Monarch Platform (Auris Health, Redwood City, CA, USA), which is a commercial tendon-driven platform for bronchoscopy, and ⑥ concentric tube robots. *(② Images courtesy of Intuitive Surgical, Sunnyvale, CA, USA ©. ⑤ Images courtesy of Auris Health ©). ⑥ Images courtesy of Dupont et al. and Butler et al. ©2009 and 2012 IEEE. Taken from J. Sikorski, Magnetic Catheters: A Journey Across Orders and Scales, University of Twente, 2020.)*

In this chapter, recent results on magnetically actuated continuum robots and soft robots developed for medical applications will be detailed. It will cover topics on magnetic actuation systems, magnetic materials, variable stiffness elements, and soft robots targeting minimally invasive interventions. Medical applications such as catheterization and polypectomy will be demonstrated with examples of new robots. Related aspects such as ultrasound (US) and computed tomography (CT) imaging, as well as biocompatibility will be discussed. The discussion will start with an overview of magnetic actuation and its application within medical robotics.

2. Magnetic actuation

The technique of magnetic actuation can be applied to any object with magnetic properties. When such objects interact with a magnetic field, they experience a wrench [13]. This interaction is complex and occurs at molecular scale. However, in robotic applications, it can usually be modeled analytically by using efficient approximations based on linear algebra [14].

These approximations assume that the object with magnetic properties occupies a point-location in space. The sum of these properties across the entire nondeformable volume of that object is represented by a single vector quantity: the magnetic dipole moment $\boldsymbol{\mu} \in \mathrm{R}^3$ [15]. By generating an external field, represented as a vector $\mathbf{B} \in \mathrm{R}^3$, at the location of the object, magnetic force $\mathbf{F}_\mu \in \mathrm{R}^3$ and magnetic torque $\boldsymbol{\tau}_t \in \mathrm{R}^3$ are exerted on the object as follows:

$$\mathbf{W} = \begin{bmatrix} \mathbf{F}_\mu \\ \tau_\mu \end{bmatrix} = \begin{bmatrix} \nabla(\mathbf{B} \cdot \boldsymbol{\mu}) \\ \boldsymbol{\mu} \times \mathbf{B} \end{bmatrix} \tag{1}$$

where nabla (∇) is a gradient operator [16]. Fig. 2 provides an illustrative explanation of this phenomenon.

Magnetic interaction is versatile and can be applied for actuation in a variety of fashions, depending on the structure and desired application of the actuated system. It has gained particular attention in medical robotics due to its noncontact nature. This allows the infrastructure used for magnetic actuation—usually comprising of large permanent magnets or electromagnetic coils—to be kept outside the body of the patient. At the same time, the actuation forces and torques can be applied directly at the desired point within the structure of a robot. A large body of research uses magnetic actuation for motion control of various microrobotic agents [17,18]. Most of the classical designs of infrastructure for the generation of external magnetic fields, such as the pioneering OctoMag, come from that field [16,19]. Research on magnetic needles and endoscopes has also produced remarkable results, indicating a potential for clinically applicable solutions [20].

The idea of using magnetic interaction to actuate a flexible catheter is not new [21]. The most conventional realization of this method involves integrating permanent magnets close to the tip of the device. By using a source of variable external magnetic field, such a catheter can be deflected in a given direction [22–24]. Other prominent types of magnetic catheters are designed to work in static external field of the MR scanner. MR-compatible catheters employ electromagnetic coils with different geometries integrated onto its body. Directional motion is achieved by activating a particular combination of coils to generate a variable dipole moment, dependent on the orientation of the catheter with respect to the external field [25].

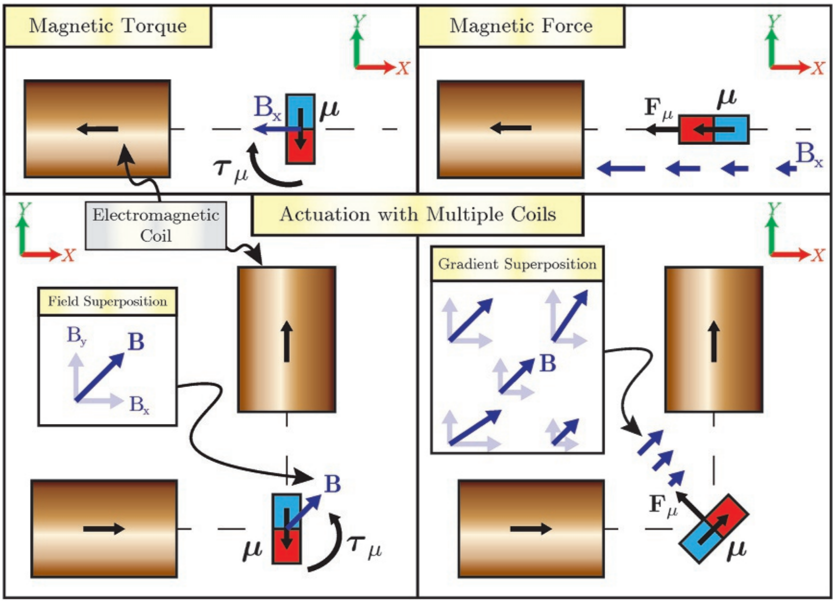

FIG. 2 Any object with magnetic properties experiences force and torque when placed in external magnetic field. Misalignment of dipoles in a magnetic field produces torque, while magnetic forces are generated by field gradient. As both magnetic fields and gradients superpose at any location, multiple magnetic field sources can be used to determine the total field and spatial gradient at a location of the object. This way, prescribed forces and torques can be exerted on the actuated object. This allows for control of both the position and the orientation of an object in a noncontact manner. *(Taken from J. Sikorski, Magnetic Catheters: A Journey Across Orders and Scales, University of Twente, 2020.)*

A few commercial solutions involving magnetically actuated catheters have been developed across the past two decades. The most successful of them is Niobe (Stereotaxis, St. Louis, MO, USA). Niobe is a system for remote guidance of magnetic catheters during cardiac ablation by utilizing two large electromagnets to generate an external field deflecting the catheter tip [26]. The direction of the field is controlled directly by the clinician, who monitors the position of the catheter using fluoroscopy. A recent metaanalysis has demonstrated distinct advantages of Niobe in cardiac ablation, reporting almost 50% lower risk of complications with respect to standard catheterization [27]. Furthermore, the reduced size and improved dexterity of the catheters actuated by Niobe makes them a viable solution for challenging coronary interventions in small and torturous vessels. However, other studies indicate that procedures performed using Niobe suffer from significantly longer execution time than conventional methods [28,29]. Recently, an improved version of the Niobe system, named Genesis, has been proposed by Stereotaxis and has received FDA approval for clinical use.

In literature, different configurations of magnetic actuation systems have been designed based on application requirements. Such systems employ stationary electromagnets [16,30], mobile electromagnets [31,32], or mobile permanent magnets [20], as sources of the magnetic field. The mobile actuation systems have the advantage of an open and typically larger workspace than stationary systems while requiring smaller external magnets [33]. For all methods, precise magnetic field information from each field source is required for actuation. Previously used approaches model the magnetic field either using an arbitrary function and fit unknown coefficients with least squares optimization [31,34], or use a first-order dipole approximation [20]. The former approach does not typically enforce constraints on the spatial gradients of the magnetic field, and the latter ignores higher order field effects that are more prominent closer to the field source [15]. A recently used approach, which solves the aforementioned disadvantages, is to express the magnetic field as the gradient of a scalar potential (scalar harmonic function), and use measurement-informed least squares optimization to fit unknown coefficients [35].

2.1 Example: Orientation control of discrete magnets in a continuum

The technical aspects of magnetic actuation, in particular with regards to field generation and application of mechanical loads on magnetic components, can be seen in Ref. [36]. Here, an approach for closed-loop multipoint orientation control of discretely magnetized continuum manipulators (CMs) is presented.

A CM with two magnetic segments and two flexible segments is suspended horizontally within the workspace, visualized using a stereo vision setup, and actuated with a magnetic field generated by electromagnets with currents. The CM magnet poses are measured with stereo vision, and the measured poses and actuation parameters are used to compute magnetic wrenches acting on the CM. An orientation Jacobian is computed that maps incremental changes in currents to changes in CM magnet orientations. Finally, the CM magnets are steered toward a desired orientation by updating the actuation parameters, namely, the currents in the coils and the positions of the coils. The control scheme (Fig. 3) is divided into four blocks (*A–D*).

A magnetic field model is used to accurately describe the magnetic field and field gradients required for computing the exerted magnetic torques and forces. In addition, a quasistatic Cosserat rod model of the CM was able to predict the magnet orientation changes in a varying nonhomogeneous magnetic field. Both the field and Cosserat rod models were applied to construct a numerically computed orientation Jacobian to linearize changes in actuation parameters to changes in magnet orientations. In the end, the presented control strategy has shown able to achieve accurate independent orientation control of two permanent magnets in experiments with six moving coils, and in 3D simulation using an extended virtual clone the experiment setup.

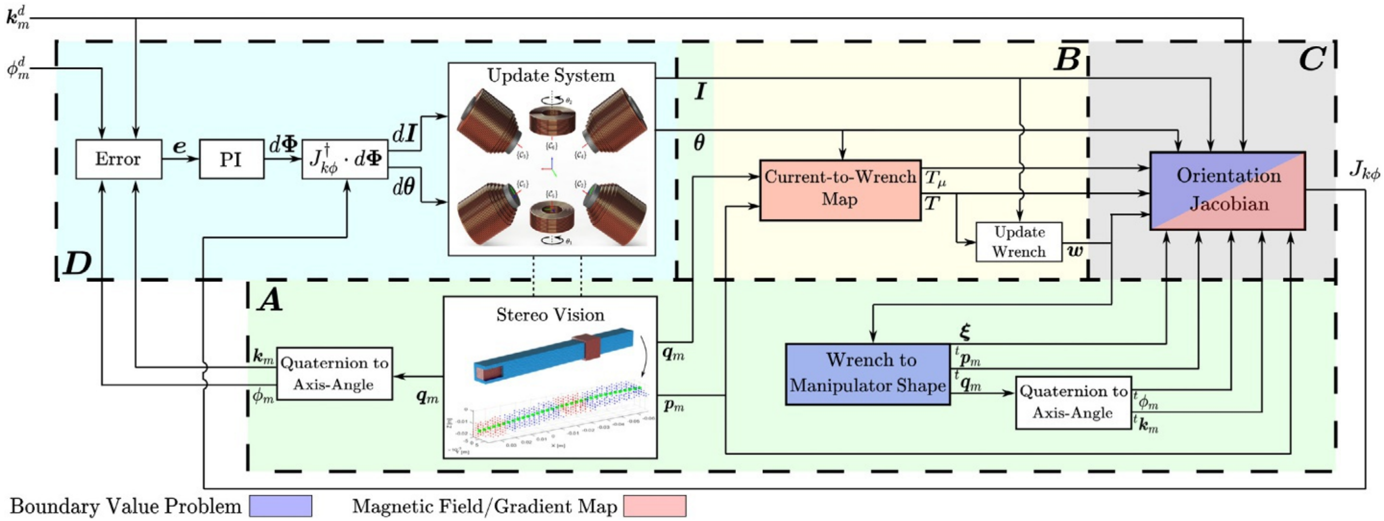

FIG. 3 Orientation control diagram. (*A*) A stereo vision setup records a 3D point cloud of the continuum manipulator (CM) that holds information about the measured magnet poses $\{p_m, q_m\}$. Knowledge of the magnetic wrench (w) acting on the magnets is used to solve the CM statics (shape) with a Cosserat rod model, which holds information about theoretical magnet poses $\{{}^t p_m, {}^t q_m\}$. (*B*) Measured magnet poses and electromagnet currents and positions $\{I, \theta\}$ of the system are used to compute the magnetic wrench. (*C*) An orientation Jacobian ($J_{k\phi}$) is computed that maps incremental changes in $\{I, \theta\}$ to changes in magnet orientations. (*D*) The orientation Jacobian and error between desired and measured magnet orientation are used to update $\{I, \theta\}$. *(Taken from M. Richter, V.K. Venkiteswaran, S. Misra, Multi-point orientation control of discretely-magnetized continuum manipulators, IEEE Robot. Autom. Lett. 6 (2) (2021) 3607–3614.)*

Fig. 4 provides side views of time-evolved shapes of the CM during the experiment. These experiments and simulations showed that it is possible to achieve convergence of multiple magnets to desired orientations by generating a nonhomogeneous magnetic field. However, when moving to practice, there are some limitations. First, the large multicoil magnetic actuation systems

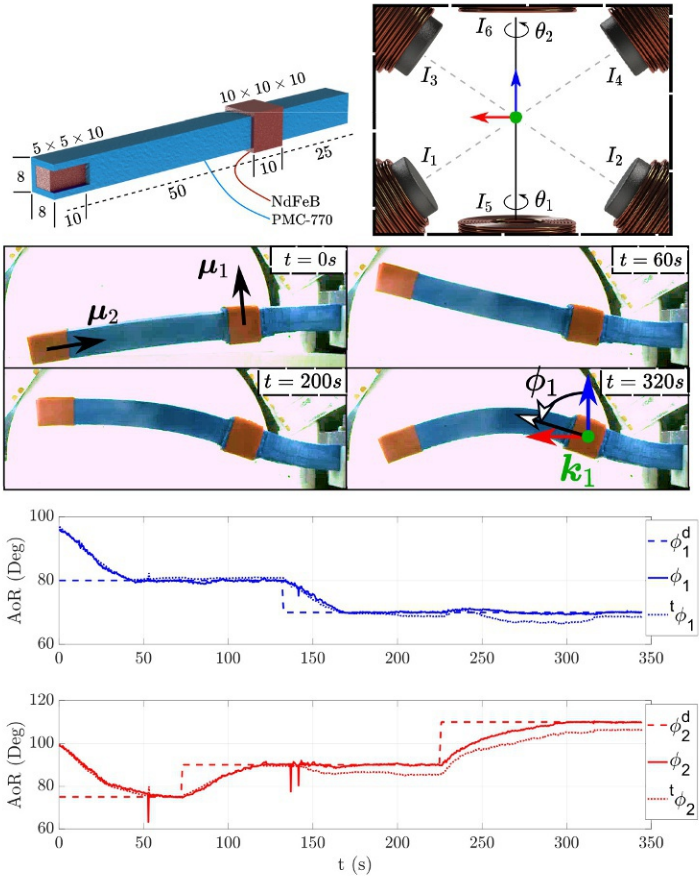

FIG. 4 Model of the continuum manipulator (CM) consisting of flexible polyurethane rubber (PMC-770) and rigid neodymium magnets (NdFeB), with dimensions given in millimeters. The magnet dipole moments, μ_m, are shown at $t = 0$s. Magnet angles of rotation (AoR) are measured relative to the global $\hat{z}$ axis, superimposed on the magnet center, shown at $t = 320$s. The CM is actuated inside the workspace of BigMag in plane with six electromagnets. Side views of time-evolved shapes of the continuum manipulator are shown and desired, ϕ^d, measured ϕ_m, and predicted, $^t\phi_m$, AoR are plot for magnet 1 (blue) and 2 (red) in degrees against time t. *(Taken from M. Richter, V.K. Venkiteswaran, S. Misra, Multi-point orientation control of discretely-magnetized continuum manipulators, IEEE Robot. Autom. Lett. 6 (2) (2021) 3607–3614.)*

are infeasible due to their small and generally immobile workspace. These systems are therefore ideally substituted for systems with fewer coils and more spatial degrees of freedom. Second, the computational cost of shape reconstruction and the Jacobian limited the control frequency, suggesting challenges to achieve closed-loop control.

3. Magnetically actuated continuum robots

The field of continuum robots has seen significant growth in the past few decades. The designs of snakes, elephant trunks, and octopus tentacles have encouraged researchers to devise bioinspired hyper-redundant robots for dexterous manipulation of objects [37]. Continuum robots have great potential within medical applications, and in particular for robot-assisted MIS. In current literature, the focus is on designing miniaturized manipulators which are sufficiently flexible to be steered inside the body and reach difficult-to-access surgical sites with high dexterity. Such devices find applications in neurosurgery, endoscopy, laparoscopy, biopsy, and other surgical procedures in which these devices enter the body through small incisions [38,39].

Recently, magnetic actuation is gaining interest in creating miniaturized manipulator designs as it enables manipulator control without the need for cables or tendons. For instance, a 4-mm flexible catheter (NaviStar-RMT, Biosense Webster, Inc., California, USA) integrated with small permanent magnets, controlled using the Niobe magnetic navigation system (Stereotaxis Inc., Missouri, USA) and a motor drive (Cardiodrive, Stereotaxis, Inc., USA), is a leading technology for cardiovascular interventions [40]. Kratchman et al. demonstrated 3D tip trajectory planning of a magnet-tipped rod using Kirchoff elastic rod model in open-loop [41]. Model-based closed-loop control has been studied by many researchers using feedback of actuating wrenches [42]. For instance, the first 3D closed loop control of a magnetic catheter was demonstrated by Edelmann et al. using Cosserat rod model; however, an external camera-based localization was implemented which is not clinically feasible [23].

Magnetized CMs can be discretely or continuously magnetized. Discretely magnetized CMs contain rigid magnetic, and flexible nonmagnetic material. The rigid magnetic material can be divided into actively magnetized electromagnets [43], or permanent magnets [20]. Alternatively, continuously magnetized CMs consist of magnetic composite polymers [44]. These can be used to fabricate specialized magnetization profiles for target applications [45,46]. The magnetized CMs deform due to a magnetic wrench, exerted by an external magnetic field. A theoretical minimum of seven magnetic DOFs is required for wrench control. However, these systems may suffer from magnet orientation-dependent singularities. By instead providing eight magnetic DOFs such singularities are avoided [14].

3.1 Catheters as continuum robots

Catheters find medical uses due to their inherent safety. Their compliance matches that of soft tissues. This allows the catheters to be inserted into the cavities of the human body with low risk of tissue damage. For manual operation, stiffer catheters are usually preferred due to their increased pushability [47]. Originally, simple catheters with a hollow lumen inside were used for drainage of body liquids or delivery of drugs into the bloodstream [48]. In recent years, more structurally and functionally complex catheters gained wide acceptance as an established class of instruments for MIS [49].

The success of currently established catheterization techniques drives the motivation for a wider adoption of this class of instruments within MIS, also outside cardiovascular applications [50,51]. However, performing a procedure with such a flexible instrument is challenging. When the catheter insertion depth increases, clinicians gradually lose the ability to control the motion of catheter tip by operating at the insertion port, due to interaction of the deformable, compliant structure of the catheter with the environment along its entire length within the body [47].

Regardless of the applied actuation technique, manual operation of steerable catheters is still challenging due to limited information available to the clinician regarding the state of the device and its pose with respect to body tissues. Thus, even the execution of standard MIS procedures involving catheters requires clinicians with extensive experience, limiting the accessibility of treatment [52]. The dexterity of steerable catheters is further degraded by the presence of unpredictable biological forces. Thus, robotic technology has increasingly been used to enhance the capabilities of clinicians to control steerable catheters, resulting in improved in vivo behavior [53,54]. Additionally, robotically steered catheters can potentially be used in places where manual operation is considered too dangerous due to delicate structures, such as in neurosurgical procedures [55].

Magnetic actuation of catheters enables simple structure with no moving components, which allows for substantial miniaturization [56]. They are actuated through a process, which can be modeled precisely and efficiently [35]. Their complex mechanical behavior gives them potential dexterity suitable for a wide range of applications [45]. For successful operation, magnetic catheters require reliable auxiliary infrastructure, capable of generating magnetic field in a clinically relevant workspace. This problem can be approached in a multitude of fashions, but it is nontrivial to solve due to the unfavorable scaling properties of magnetic fields. For that reason, the systems designed for workspaces encompassing entire human body are large and bulky, have high power demands, and offer relatively low actuation bandwidth. As an alternative, systems with smaller workspaces are commonly used, usually employing stationary electromagnetic coils. This trend has been initiated by the OctoMag system, originally intended for actuation of microrobotic agents in eye surgery applications, and since then used also in a handful of studies on magnetic catheters

[16,57]. Another method uses mobile permanent magnets to guide catheters and endoscopes [41,58–60].

Conventional research on magnetic catheters aims at increasing precision during conventional MIS procedures. Additionally, several functionalized magnetic catheters have been proposed predominantly for tasks involving removal of tissue using incisions or ablation [56,61]. These relatively modest applications neither exhaust the potential of magnetic catheters nor provide convincing justification for regular clinical use of them, as the complex auxiliary infrastructure required involves large capital costs. The advances in the domain of untethered milli/microrobotics indicate that magnetic actuation can be used to create significantly more advanced devices [62,63]. The rapidly evolving field of soft robotics has also demonstrated that by smart use of magnetic elements, rich behavior of flexible elements can be achieved [46,64–66].

3.2 Flexure-based continuum manipulators

Continuum manipulators can also be designed out of discrete flexible components. Here, the functionality of the manipulator is tied to the mechanical behavior of the individual components. Flexure-based designs with reduced stress and limited local deformation have potential for application in design of surgical devices. For instance, Swaney et al. [67] have designed a flexure-based steerable needle that minimizes tissue damage, and Chandrasekaran et al. [68,69] have developed flexure-based designs of surgical tooltip combined with magnetic coupling and tether-driven power transmission. Kim et al. have designed a continuum manipulator using creative slotting patterns of narrow necked flexures resulting in discrete compliance [70]. Flexure-based designs are also found in the backbone structures of endoscopic continuum robot designed by Kato et al. [71] and the Artisan Extend Control Catheter by Hansen Medical, Inc. (California, U.S.) [72], which are tendon-driven devices.

In Refs. [73,74], a new design of a metallic compliant continuum manipulator capable of planar and spatial bending is presented. The design entails a novel slotting pattern to make a segmented continuum manipulator that is capable of bending about two axes and is cut out of a monolithic tube without using assembly. The monolithic compliant design of manipulator enables easy modeling due to linear load-deformation characteristics at individual segments of the manipulator. The manipulator has built-in mechanical motion constraints which restrict the maximum stress in the flexure, thereby ensuring safety of the manipulator during use. The manipulator is actuated using controlled magnetic fields by attaching a permanent magnet at its tip.

The miniaturized manipulator presented is fabricated using a single tube of titanium, thus eliminating the need for assembly. The mechanical motion constraints in the design lead to a safe manipulator by preventing the flexures from failing under stress. The 1-mm working channel of the manipulator enables integration of additional tools and sensors. The clinical feasibility of the manipulator is studied by carrying out experiments using a miniature camera (0.91 mm diameter) in phantom models of a bifurcating arterial system and a heart. Magnetic steering of the manipulator integrated with a miniature camera as feedback shows potential as a steerable catheter for endoscopy and ablation.

The manipulator is fabricated using a titanium (grade-2) tube of outer and inner diameters of 3 and 1 mm, respectively. Titanium (grade-2) is chosen as the material as it has high ratio of yield strength to elastic modulus ($\sigma_y = 345\,\text{MPa}$ and $E = 105\,\text{GPa}$) and low weight ratio. It is biocompatible and magnetically transparent. A series of flexure pairs is created along the length of the manipulator by making cuts using wire electrical discharge machining (EDM). The manipulator is actuated using magnetic fields by means of a permanent magnet attached to its tip (Fig. 5B).

Magnetic steering of the manipulator is demonstrated inside the undulating tapered channels of a bifurcating arterial phantom. The experiment is performed by positioning the phantom in vertical and horizontal orientations as shown in Fig. 6A and B. In a second experiment, the maneuverability of the manipulator is tested inside a heart model. The manipulator is inserted through the aortic valve and is guided to reach three targets locations in the left ventricle (Fig. 6C). A miniature camera is embedded within the working channel of the manipulator and demonstrates the steerability of the manipulator without relying on an external imaging system.

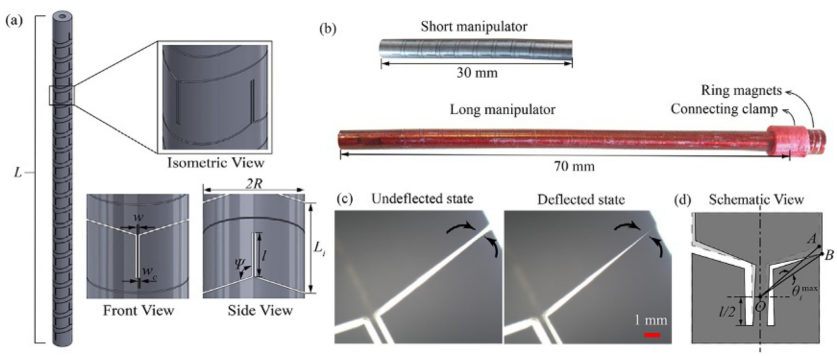

FIG. 5 (A) The isometric, top, front, and side views of two-axis bending design of manipulator with variables to define the design parameters. (B) Short and long versions of the manipulators fabricated using wire EDM. Three neodymium ring magnets are connected to the long manipulator which is colored red for stereo vision tracking purposes. (C) Microscopic images of one flexure joint of the manipulator undergoing maximum deflection. (D) A schematic view of a flexure pair undergoing maximum deflection. *(Taken from T.L. Thomas, J. Sikorski, G. Ananthasuresh, V.K. Venkiteswaran, S. Misra, Design, sensing, and control of a magnetic compliant continuum manipulator, IEEE Trans. Med. Robot. Bionics (2022) 1.)*

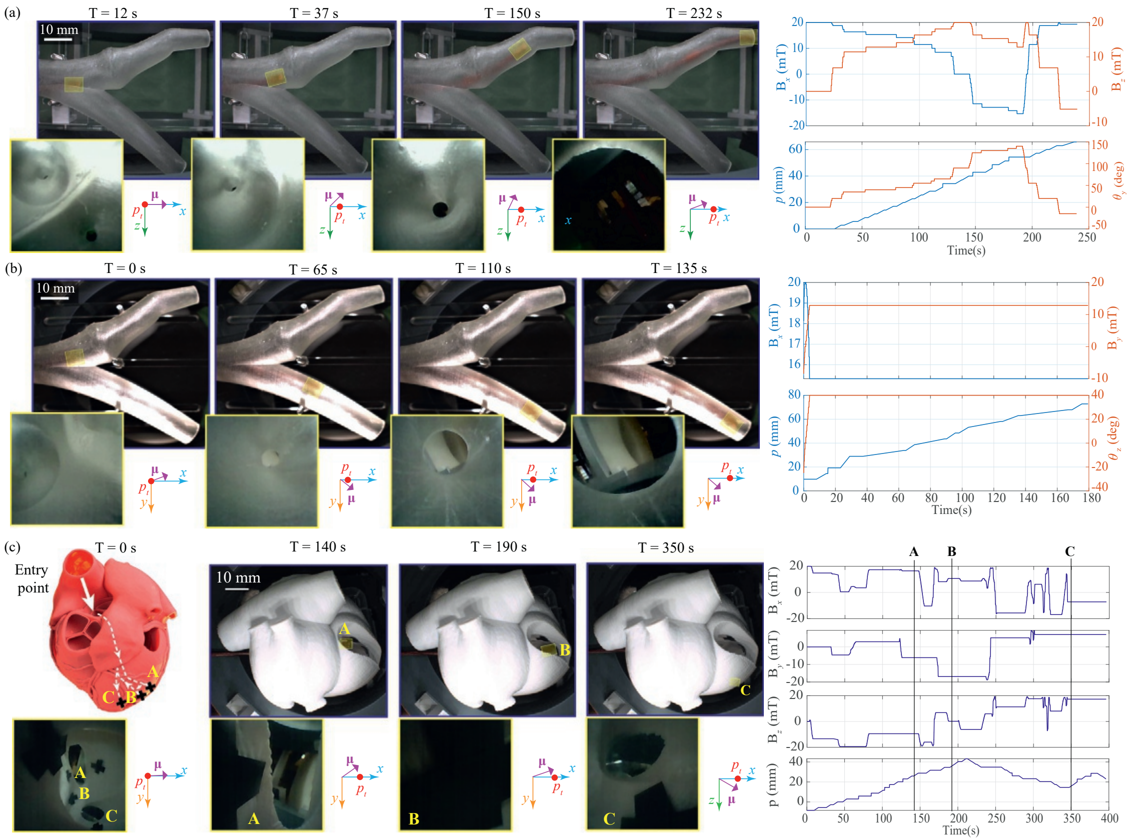

FIG. 6 (A and B) Manipulator guidance inside a bifurcating arterial phantom suspended vertically and horizontally in the workspace of a magnetic actuation system. (C) Manipulator guidance inside a heart model. The dotted white lines show the traced trajectory starting at the aortic valve to reach three target locations A, B, and C in the left ventricle. Plots show generated magnetic field (B_x, B_y, B_z), its direction (θ_y, θ_z), and manipulator insertion (p). *(Taken from T.L. Thomas, J. Sikorski, G. Ananthasuresh, V.K. Venkiteswaran, S. Misra, Design, sensing, and control of a magnetic compliant continuum manipulator, IEEE Trans. Med. Robot. Bionics (2022) 1.)*

3.3 Soft materials-based continuum manipulators

Magnetic characteristics can also be incorporated into soft materials to form what are called magnetic polymer composite (MPC) [44,75]. MPC consists of magnetic microparticles suspended in an elastomer base. The volume fraction of magnetic particles as well as their magnetization profile can be predefined to achieve preprogrammed behavior of MPC robots [76–78]. As such, a wide range of motion may be achieved in an external magnetic field [45,46,79].

Magnetic continuum manipulators (MCMs) are continuum flexible robots which can be actuated using magnetic fields. Although the material used in MCMs can vary, most designs have a slender cylindrical geometry and use either rigid magnets or MPC. For slender designs, i.e., where the MCM length is significantly bigger than the diameter, magnetic volume and moment decreases. Reducing magnetic moment decreases the magnitude of exerted magnetic forces and torques. The gained flexibility inherent to a slender design compensates for the reduction in torque [56,63], but at the cost of reduction in actuation force [32,80].

Material properties that affect magnetic moment are (average) magnetization and volume. For cylindrical MCMs, magnetic moment and bending stiffness scale with the second and fourth power of radius, respectively. Magnetization scales linearly with magnetic volume fraction, but at an exponential cost in bending stiffness. Therefore, bending stiffness increases at higher rate than magnetic moment with diameter. Stiffness can be partially compensated by interaction between internal magnets, i.e., local dipole interactions, which cause forces and torques exerted between segments of the MCM to affect its elasticity [81].

In Ref. [82], an MCM design is presented to enable increasing diameter without compromising on bending flexibility, magnetic moment, and thereby magnetic pulling forces. The proposed design combines MPC single helices with intermittent permanent ring magnets, assembled over a flexible tube. A segment comprises two ring magnets and an MPC helix shaped as a cored closed and ground compression spring (Fig. 7A). Ring magnets have predetermined length (L_{mag}). The helix contains a suspension of praseodymium-iron-boron microparticles (PrFeB) and polydimethylsiloxane (PDMS).

To analyze the local dipole interactions between multiple ring magnets in an MCM, the interaction between 2 and 5 ring magnets at various relative angles is simulated. Bending torques on the tip magnet due to the collective field and field gradients of preceding magnets are computed. MCM maneuverability is shown in a phantom representing the human adult abdominal aorta and compared to an MPC cylinder (0.2 volume fraction). An external magnet is manually moved beneath the phantom (Fig. 8A) at a 30–40 mm distance. The phantom trajectory includes bifurcations with angles up to 135°. The MCM (Fig. 8B) takes on J- and S-shaped forms where the MPC-rod is unable to.

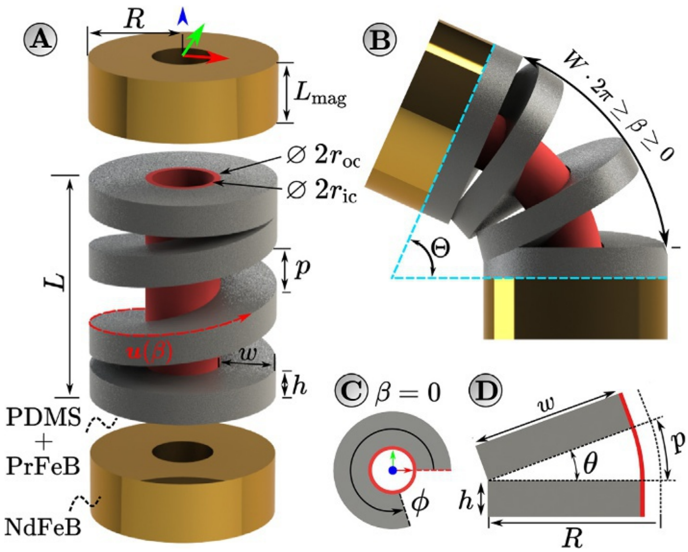

FIG. 7 Design of a magnetic segment of an MCM. Ⓐ Segments are made from magnetic polymer composite (MPC) and neodymium-iron-boron (NdFeB) ring magnets. MPC contains a suspension of polydimethylsiloxane (PDMS) and praseodymium-iron-boron (PrFeB) microparticles. The MPC is shaped as a closed and ground compression spring (gray) with a core cylinder (red). Ⓑ Segment bending is limited to a boundary deflection angle (Θ). The helical part of the spring is described by revolution angle (β). Ⓒ Transverse cross-section of the helix. The core cylinder is shown with the red circle. MPC surrounds the cylinder with a sector angle (ϕ). Ⓓ Single pitch bending. With each pitch, the helix can bend with $\theta = \Theta/W$ before adjacent windings touch. *(Taken from M. Richter, M. Kaya, J. Sikorski, L. Abelmann, V. Kalpathy Venkiteswaran, S. Misra, Magnetic soft helical manipulators with local dipole interactions for flexibility and forces, Soft Robot. (2023).)*

Additionally, to show medical application, the MCM is steered from the left common iliac to the superior mesenteric artery where a contrast dye simulant (water with red dye) is released (Fig. 8C). The simulant is injected with a syringe through the free-hanging backbone from outside the phantom. Then, with the peristaltic pump turned on (flow of 2.7 L/min) the MCM is navigated through the phantom (total path length >50 cm) within 1 min (Fig. 8D). Additionally, the backbone may be used as a guiding sheath for, e.g., guidewires to reach distal vessel bifurcations (Fig. 8E). In the future, actuation can be improved by teleoperation of robotically moved external magnets. Additionally, imaging may be performed with, e.g., C-arm fluoroscopy [83].

These demonstrations are performed in a 2D phantom. One of the factors that need to be considered for 3D navigation is MCM weight. Insertion into vasculature also requires an introducer sheath, which could be combined with manual or robotic insertion. The demonstrations are performed in a vascular phantom to illustrate the spatial confinement, nonlinear paths, and sharp turns. The design principles presented may be translated to other medical and nonmedical environments.

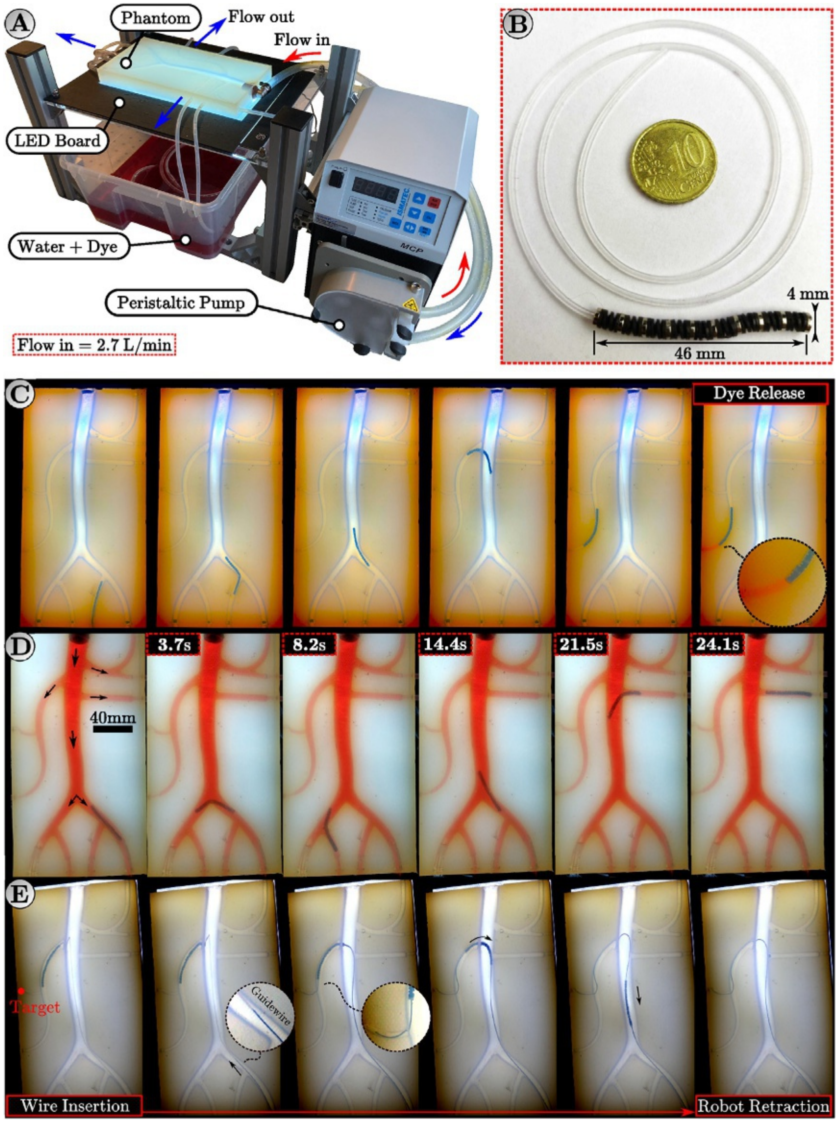

FIG. 8 Navigation experiments with an MCM. Ⓐ Experimental setup. Ⓑ Assembled MCM. Ⓒ MCM maneuvering to inject contrast dye using a handheld permanent magnet at a distance of 30–40 mm. Ⓓ MCM maneuvering with the peristaltic pump turned on. Ⓔ Passing a guidewire through MCM backbone. *(Taken from M. Richter, M. Kaya, J. Sikorski, L. Abelmann, V. Kalpathy Venkiteswaran, S. Misra, Magnetic soft helical manipulators with local dipole interactions for flexibility and forces, Soft Robot. (2023).)*

3.4 Variable stiffness manipulators

Variable stiffness in surgical manipulators has been gaining significant attention in recent years. Several studies have investigated different mechanisms to achieve variable stiffness such as granular/particle jamming, antagonistic arrangement of actuators, and stimuli-responsive stiffness-tunable materials [84]. A variable stiffness mechanism based on fiber jamming transition was introduced in the STIFF-FLOP soft manipulator to provide stability to its distal module by making it rigid; however, miniaturization of this technology proved to be challenging [85]. A lightweight re-configurable stiffness-changing skin based on layer jamming was created and adopted as on-demand joints for a continuum manipulator enabling dynamic adjustment of the operating workspace [86]. Cable-driven actuators [87] and fluidic actuators [88] are commonly used in antagonistic methods but are limited by low range of stiffness variation and controllability when it comes to MIS [89].

Stiffness-tunable materials such as low melting point alloys (LMPAs), shape memory alloys (SMAs), and shape memory polymers (SMPs) can attain significant stiffness change [80,90–93]. Despite the toxic nature of LMPA, owing to its transition speed, it has been used in the multisegment designs of a cable-driven continuum manipulator for MIS application [91], and magnetic variable stiffness catheters for applications in cardiac ablation and robotic ophthalmic surgery [80,94]. SMAs have high power-to-weight ratio, are biocompatible, easy to miniaturize, and can be activated using Joule heating [95]. Therefore, SMA wires in the form of springs, strips, and wavy patterns have been used in the design of continuum manipulators for actuation and variable stiffness [92,96,97]. However, SMAs exhibit relatively lower range of stiffness change than SMPs, a limitation that could be solved by combining with a thermoplastic [98]. SMPs are versatile due to their compatibility with 3D printing and multimaterial fabrication. Material synthesis enables developing multi SMP, that is, SMP with two or more transition temperatures, manifesting improved mechanical properties and recoverability [99,100]. Recently, SMP was used in the design of magnetic variable stiffness catheters in which graphite, neodymium, and carbon black particles were incorporated in the SMP composite to improve the electrical and thermal conductive properties [93,101].

In Ref. [102], a VSM is developed with a backbone made of a silicone tube enclosed within a spring made of SMP and a permanent ring magnet attached to its tip. The SMP spring is embedded with a resistive wire to heat the SMP by passing current. The SMP spring in rigid phase is initially in a compressed state resulting in a minimum length of the VSM, and it can be moved to a target location in its compact form. When the SMP is activated by heating, it transitions to the soft phase, and by pushing the silicone tube, the VSM is extended in length. The orientation of the VSM tip with magnet is controlled with the application of a bending moment resulting from external magnetic fields. The VSM can be deflected to extend or bend while the SMP is in soft phase, and its shape can be fixed when the SMP transitions to rigid phase. A two-segment design of the VSM can be formed using two SMP springs in series enclosing a two segment concentric tube backbone of silicone (Fig. 9A). Various bending configurations can be achieved with selective activation, bending and extension of the VSM segments (Fig. 9B). The stiffness change of the SMP when transitioning between the soft and rigid phases enables fixing the shape of the VSM (Fig. 9C), which is controlled under magnetic actuation.

The variable stiffness in the VSM is activated by means of Joule heating. The SMP used in the design has a glass transition temperature of 35°C, below which it is in glass phase, and at 60°C, it reaches the rubber phase. The SMP spring wire is embedded with a nichrome wire of diameter 0.12 mm running through the cross section of the SMP spring wire twice, with the two ends of the nichrome wire leaving the end of the SMP spring wire to connect to a power supply.

Potential clinical applications of the VSM as a steerable surgical manipulator are demonstrated with one-segment and two-segment designs. A permanent magnet attached to the end-effector of a robotic arm is programmed to generate the required magnetic field to control the VSM. The one-segment VSM is used to demonstrate endoscopy and biopsy procedure in a stomach phantom having polyps. In the first experiment, a miniature camera (0.91 mm in diameter) is integrated in the working channel of the one-segment VSM and tested in a stomach phantom. The one-segment VSM is inserted through the esophagus in its compressed form while in glass phase, and upon entering the stomach, the VSM is extended in length by activating the SMP to rubber phase. The VSM is deflected in rubber phase with the application of magnetic fields using the robot arm while manually controlling its length to scan the volume of the stomach and detect the three polyps. Fig. 10A depicts the endoscopy procedure carried out by the one-segment VSM and the view through the miniature camera of the polyps inside the stomach. In the second experiment, a cold snare polypectomy tool is integrated in the working channel of the one-segment VSM. As shown in Fig. 10B, the one-segment VSM is inserted to reach the polyp similar to the first experiment. Thereafter, the VSM is locked in position using the magnetic field while the SMP transitions to glass phase, and the snare is deployed to grasp the polyp. The polyp is resected by retracting the snare, and the SMP is activated to rubber phase. The VSM is finally retracted to its compressed form for subsequent withdrawal through the esophagus.

The maneuverability and shape fixity of the two-segment VSM is demonstrated by navigating it through three rings distinctly oriented in 3D. An optical fiber is integrated in the working channel of the VSM to transmit laser light. As shown in Fig. 10C, the VSM enters the first ring in its compact form, in which both the distal and proximal segments known as segments 1 and 2 are in fully compressed states while in glass phase. Through successive heating and cooling of each segment, the VSM is steered through the three rings. The VSM is retracted back through the three rings following the whole process in reverse

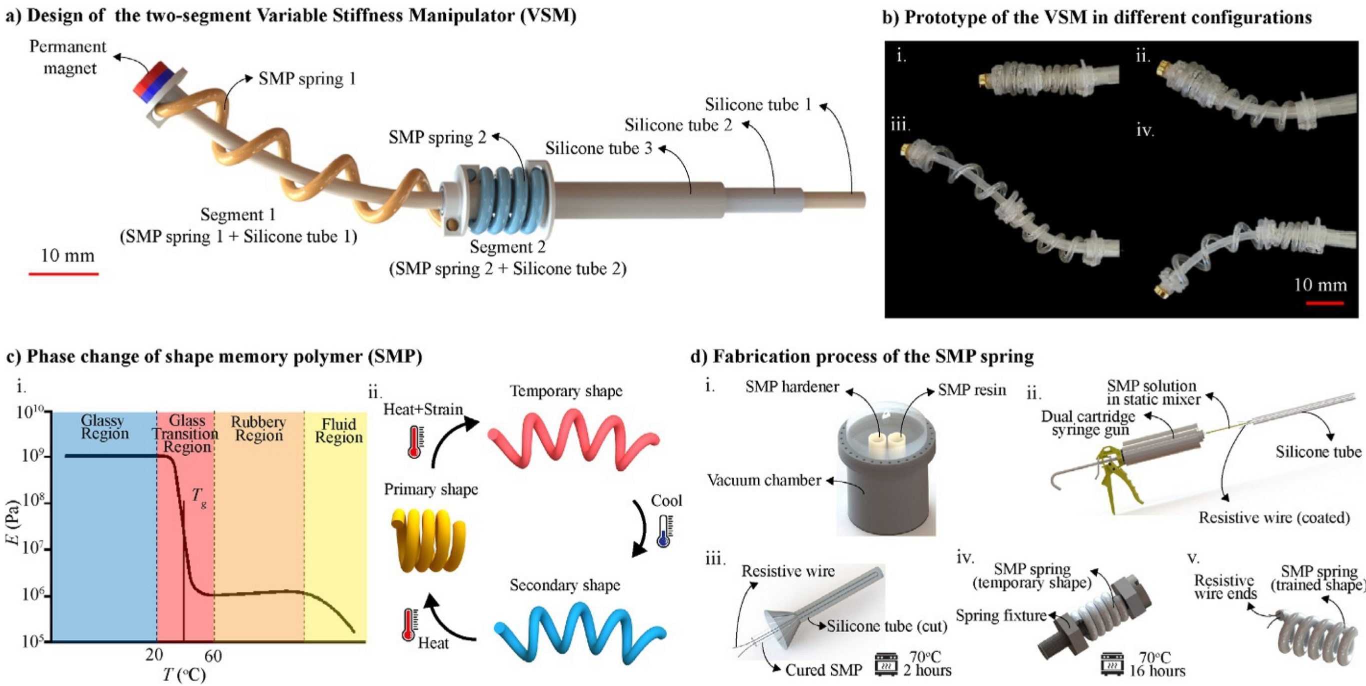

FIG. 9 (A) An illustration of the design of a two-segment variable stiffness manipulator (VSM). (B) Fabricated prototype of the VSM in different bending and extension configurations. (C) Phase change of shape memory polymer (SMP): (i) Plot of elastic modulus (E) versus temperature (T) of the SMP with glass transition temperature T_g. (ii) Shape memory effect illustrated for an SMP spring. (D) Fabrication process of the SMP spring: (i) Vacuum drying of the SMP resin and hardener for 2 h. (ii) Injection of the mixed SMP solution into a silicone tube with a coated resistive wire. (iii) Curing of the silicone mold in an oven at 70°C for 2 h and demolding the cured SMP from the silicone mold. (iv) Fixing the SMP wire into a temporary shape of the spring and training the SMP spring in the oven two cycles of 70°C for 16 h. (v) The trained SMP spring. *(Taken from T.L. Thomas, J. Bos, J.J. Huaroto, V. Kalpathy Venkiteswaran, S. Misra, A magnetically actuated variable stiffness manipulator based on deployable shape memory polymer springs, Adv. Intell. Syst. (2023) 2200465. https://onlinelibrary.wiley.com/doi/pdf/10.1002/aisy.202200465.)*

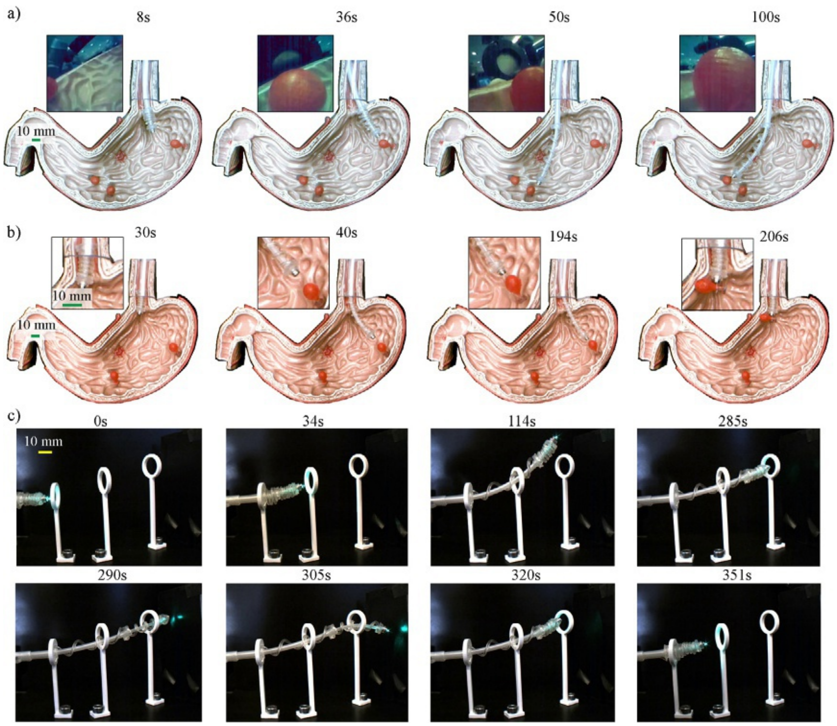

FIG. 10 Demonstration of endoscopy, biopsy, and laser ablation applications using a variable stiffness manipulator (VSM): (A) One-segment VSM integrated with a miniature camera guided inside a stomach phantom using robotic magnetic actuation to detect the three polyps. The inset shows the miniature camera view. (B) One-segment VSM integrated with a cold snare removes one of the polyps in the inner lining of the stomach. The inset shows a magnified view of the VSM. (C) Two-segment VSM integrated with an optical fiber carrying laser light is steered to navigate through three rings oriented in 3D space. *(Taken from T.L. Thomas, J. Bos, J.J. Huaroto, V. Kalpathy Venkiteswaran, S. Misra, A magnetically actuated variable stiffness manipulator based on deployable shape memory polymer springs, Adv. Intell. Syst. (2023) 2200465. https://onlinelibrary.wiley.com/doi/pdf/10.1002/aisy.202200465.)*

order. This demonstration shows the uncoupled actuation, bending, and shape locking capability of the two-segment VSM while navigating a restricted environment and transporting laser beam as a potential application for laser surgery.

4. Magnetically actuated untethered soft robots

The flexibility and controllability of soft robots have been demonstrated through diverse actuation approaches. Electrical, pneumatic, acoustic, chemical, and magnetic are currently the most widely used methods of actuation [12]. In particular, magnetic actuation shows great promise for medical applications such as magnetic catheter ablation and electromagnetic navigation bronchoscopy, owing to its benefits including human-safe operation, wireless actuation, and rapid response [103,104]. Magnetic actuation eliminates the mechanical tether between robot and actuation unit. Untethered soft robots can navigate tortuous paths better than their tethered counterparts. Thus, magnetically actuated soft robots can potentially be used for MIS, targeted drug delivery, and clinical diagnostics [10]. Magnetically actuated soft robots for medical applications are required to be functional, biocompatible as well as capable of robust motion inside organs within the human body in a myriad of environmental conditions.

Magnetically actuated soft robots (or "magnetic soft robots") are fabricated with MPCs and actuated using external magnetic sources (electromagnets or permanent magnets) [105]. Miniaturized designs capable of complex motion are made possible through the use of design-specific magnetization profiles [44,46,106]. For instance, flexible magnetic robots fabricated from a single strip of MPC have successfully demonstrated swimming motion, flagella-based propulsion, rolling, jumping, and other methods of locomotion [107–109]. Magnetic soft robots are particularly suited to medical applications because magnetic fields are not harmful to humans, and these robots can potentially be imaged and controlled using clinically relevant techniques such as magnetic resonance imaging (MRI) [57,110,111]. Recent developments have focused on improving fabrication techniques for magnetic soft robots to produce a variety of shape changes and deformation modes [66,76,112]. Untethered microscale grippers actuated using magnetic fields have been developed by many groups while also incorporating responses to other stimuli (heat, light, chemical reagents) [113–117]. Manipulation of target objects in 3D in a liquid medium has been demonstrated using untethered grippers actuated through a combination of magnetic forces and magnetic torques [118,119].

The rest of this chapter highlights recent developments in magnetic actuation of soft robots, and their extension toward medical applications. It will begin with studies investigating design, actuation, and control of magnetic soft robots, and then discuss updates regarding clinical aspects such as biodegradability, biocompatibility, bioadhesion, clinical imaging with US and CT, and response to other stimuli.

4.1 Bioinspired magnetic soft robots

Nature has always been a source of inspiration to humans, demonstrating a plethora of highly complex but well-optimized systems. Many organisms display a variety of motion capabilities with incredible coordination and control. Much of the research in robot locomotion is centered around biomimetics, to replicate biological motion patterns for adapting to specific environments [120]. Robots have been developed for motion on granular media and uneven terrain, flapping wing flight inspired by hummingbirds and insects, and wall-climbing robots have incorporated ideas from geckos [121–125]. Drawing inspiration from biological forms is particularly useful in the fields of milli- and microscale robotics, which require efficient functionality and high versatility with a limited amount of material.

In a preliminary study, four milli-scale soft robots were designed (Inchworm, Turtle, Quadruped and Millipede) and their actuation under external magnetic fields investigated with the objective of reproducing multilimbed motion patterns observed in nature [64]. Magnetic properties are incorporated into a silicone polymer to form the MPC by mixing in ferromagnetic microparticles (PrFeB) before curing. The MPC is used to fabricate soft magnetic parts, with predetermined magnetization profiles achieved using a 1 T field. The resulting soft robots are actuated under external magnetic fields of 10–35 mT which are controlled using an array of six electromagnetic coils.

The magnetic material used in this work is an isotropic powder made from praseodymium-iron-boron (PrFeB), with a mean particle size of 5 μm (MQFP-16-7-11277, Magnequench GmbH, Germany). Praseodymium (Pr) is a hard magnetic material (high magnetic remanence), which implies that it is capable of providing strong, permanent magnetic dipole moments (μ) once magnetized. This property is highly beneficial for magnetic actuation technique used in these robots. The polymer into which the magnetic particles are mixed is a silicone rubber (Ecoflex00-10, Smooth-On, Inc., USA). This material also makes up the nonmagnetic parts of the soft robots. The magnetic powder is added before curing in a 1:1 ratio by mass to create the MPC. After the polymer cures, the magnetic parts are subjected to a field of 1T (B-E 25 electromagnet, Bruker Corp., USA) using fixtures to describe the magnetization profile.

Experiments for demonstrating the motion of the soft robots are performed in an array of six electromagnetic coils called BigMag [126]. Rotating magnetic fields are used to achieve the desired motion patterns. The resulting motion of the four designs is illustrated in Fig. 11. It is noticeable that all the specimens follow the characteristic biomimetic patterns. The actuation cycles are applied repeatedly, and each specimen is capable of reliably moving from one end of the workspace to the other.

In an extension of the bioinspired designs, two types of soft robots and two types of grippers were investigated [127]. The first robot is inspired by myriapods such as millipedes and centipedes, and named Millipede robot. In nature, these organisms achieve locomotion by utilizing central pattern generators (CPGs) to coordinate limb function in groups [128]. The legs of the robot are activated in a sequential metachronal rhythm, with a noticeable wave-like characteristic.

The other soft robot developed here is a six-legged robot, named Hexapod. It has an alternating tripod gait inspired by ants and other arthropods, with three pairs of legs [129,130]. Each pair of legs is antisymmetric, that is, one leg is out of phase with the other. This leads to three of the legs making contact with the ground at any point during the gait cycle, forming a tripod support. The other three legs make contact with the ground during the opposite half-phase of the gait cycle.

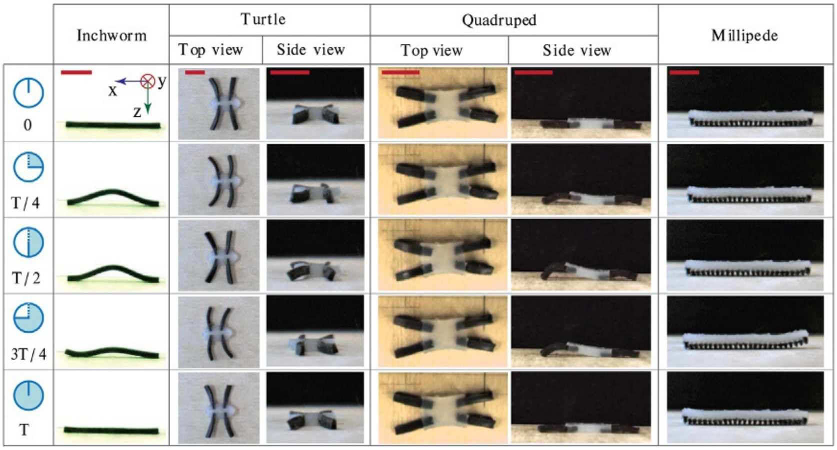

FIG. 11 The resulting motion patterns of four magnetic soft robot designs, illustrated using stills from recorded videos. Five frames from a single actuation cycle are shown for each pattern, representing various stages during the cycle (time period *T*). The coordinate system used to define the magnetic fields is shown in the top-left image, and the red scale bar denotes 10mm. *(Taken from V.K. Venkiteswaran, L.F.P. Samaniego, J. Sikorski, S. Misra, Bio-inspired terrestrial motion of magnetic soft millirobots, IEEE Robot. Automat. Lett. 4 (2019) 1753–1759.)*

In order to grant functional properties to the robots, two bioinspired gripper designs are also produced. The Tail gripper developed here is inspired by prehensile tails (seen in organisms such as new world monkeys, seahorses, and pangolins) and consists of a flat piece of magnetic silicone which can be attached to the robot. Inspiration for the second gripper design—the Flower gripper—comes from various flowering plants and organisms such as jellyfish, tapeworms, and carnivorous plants like bladderworts.

The robots and the grippers are paired such that their actuation modes are complementary to one another. The Millipede robots are paired with the Tail grippers since they are both actuated using rotating magnetic fields. The Tail grippers require higher magnetic fields rotating at a lower frequency compared to the fields required for the actuation of the Millipede robots. The Flower grippers are attached to the Hexapod robots in a configuration, which ensures that the axial direction of the gripper is along the length of the robot. Therefore, the direction of the magnetic field required for actuation of the gripper is orthogonal to the magnetic field required for actuation of the legs of the robot. This pairing ensures that the robots and grippers can function independently.

Experiments are conducted to demonstrate the maneuverability of the robots, the function of the grippers, and their combined actuation. The maneuverability of the robots is demonstrated by guiding them to a target location within the workspace while avoiding obstacles. The grasping functionality is illustrated through tasks where the robots either pick up objects from the environment or place them at target locations. The different modes of actuation are programmed into the system and controlled through teleoperation. Camera images are used by the operator to determine the position and orientation of the robots within the workspace. Images from the experiments can be seen in Fig. 12.

In these studies, magnetic actuation has been used in combination with soft materials to demonstrate bioinspired terrestrial motion of untethered millirobots. The untethered magnetic soft robots with grasping manipulators are capable of executing pick-and-place tasks. The development of small-scale, untethered soft devices could have many applications in areas where remote actuation is necessary.

4.2 Toward medical applications

Magnetic soft robots show most promise in manipulating objects in constrained or enclosed spaces in scenarios where a mechanical tether would be infeasible.

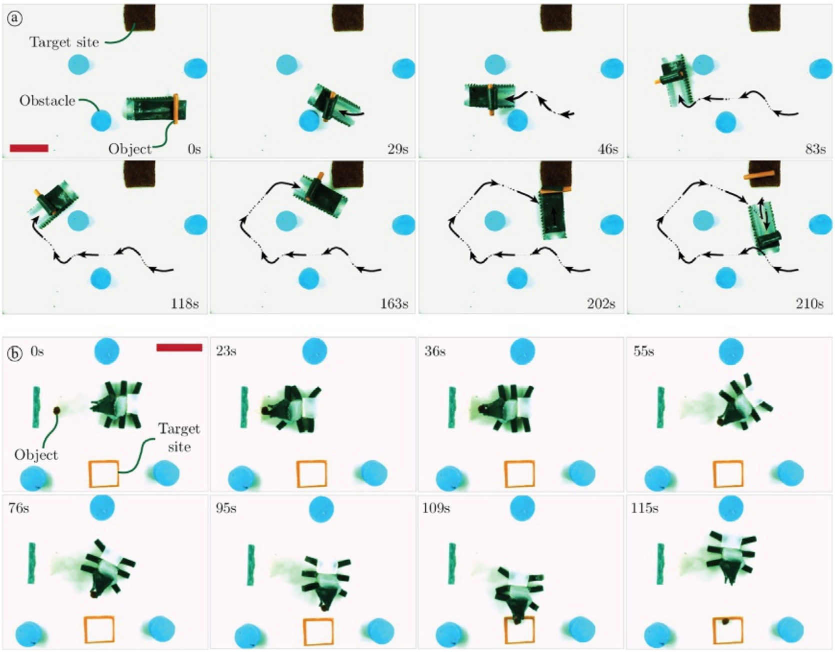

FIG. 12 ⓐ Millipede robot with Tail gripper performing a pick-and-place task. The robot first gathers the object, then navigates past obstacles to reach a target site, and deposits the object by unfurling the gripper. Scale bar is 20 mm. ⓑ Hexapod robot with Flower gripper performing a pick-and-place procedure. The robot first moves toward the object, grasps it by activating the gripper, then navigates to a target site, and deposits the object by actuating the gripper. Scale bar is 10 mm. *(Taken from V.K. Venkiteswaran, D.K. Tan, S. Misra, Tandem actuation of legged locomotion and grasping manipulation in soft robots using magnetic fields, Extreme Mech. Lett. 93 (1097) (2017).)*

One particular area of interest is minimally invasive surgical interventions, where these types of robots can be used for targeted therapeutic applications, such as biopsy and drug delivery. Miniaturization of the robots would be helpful for applications in MIS. Developments in materials and manufacturing are opening up the possibility of producing these robots at different dimension scales, including submillimeter sizes. Adding sensory elements and localization capabilities would provide the potential for autonomous control in application-relevant scenarios. The use of other smart materials within the MPC and developments in the design of electromagnetic actuation systems would also open up the range of applications for these types of soft robots. Some examples are described in the following sections.

4.2.1 Biodegradability

Biodegradable materials have been used to fabricate soft robots for safe operation inside the human body [131]. The functions of drug delivery and release of biodegradable materials have been demonstrated on microswimmers [132,133]. There are several choices for biodegradable elastomers based on polyesters or hydrogels [134,135]. A mixture of gelatin, glycerol, and water (GGW) has been verified to be soft and biodissolvable, and the constituent components are commonly available [136].

Wang et al. demonstrated a magnetically actuated soft robot with biocompatible and dissoluble components [137]. The robot body is made of four magnetic cubes joined through links made from the biodegradable mixture. The magnetic particles interact with an externally generated magnetic field to produce magnetic torques that are used for motion actuation. The robot has four cubes of MPC (not biodegradable) which enable magnetic actuation. For the biodegradable part of the robot, a mixture of gelatin, glycerol, and water (GGW) is used. This makes up the outer cover for the magnetic cubes and the links between the magnetic segments. The biodegradable mixture is flexible, and the intermediate links twist and bend, enabling snake-like motion of the robot.

The functions of the robot demonstrated here are carrying a mock-drug, being steered to a target location in the workspace and drug release through dissolution (Fig. 13). The maneuverability of the robot is demonstrated by steering the robot to correct its heading and move through an obstacle (hole in the middle wall). After moving through the hole, the robot crawls down the slope into the reservoir of water. In order to demonstrate the function of drug release, a small quantity of a mock-drug is integrated into the middle link. The mock drug is released when the middle GGW link is dissolved, staining the water with the dye. After complete dissolution of the GGW, the four magnetic cubes attract each other and form a rectangular bar. Finally, the bar of cubes is guided to one side of the workspace.

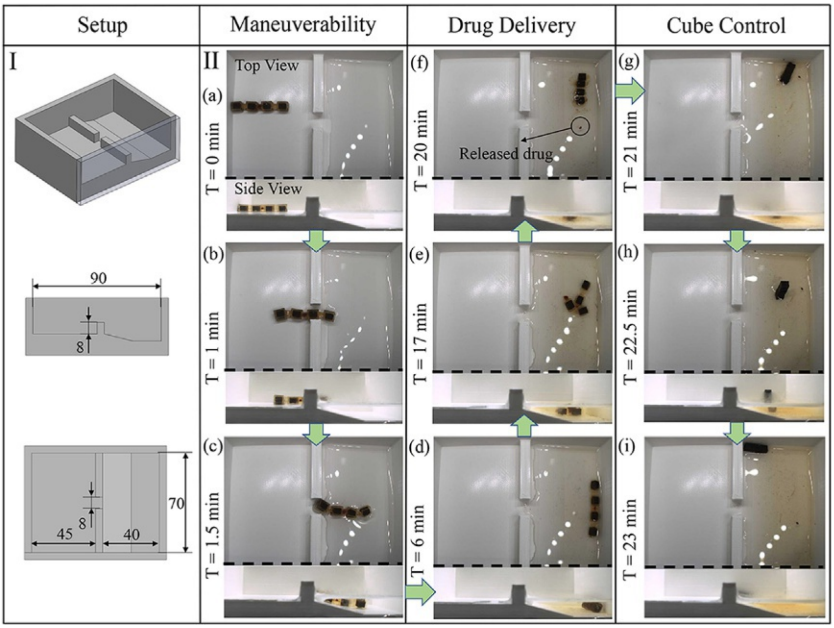

FIG. 13 Biodegradable robot functions I. Workspace for the experiment. Perspective, top, and side view are shown. Dimensions are in mm. II. Experimental results. The maneuverability of the robot is demonstrated by steering through a hole in the wall (a, b, c). The robot enters the water and rotates until the GGW links dissolve, releasing the mock-drug (d, e, f). After dissolution, the magnetic cubes are moved to one side of the workspace. *(Taken from C. Wang, V.R. Puranam, S. Misra, V.K. Venkiteswaran, A snake-inspired multi-segmented magnetic soft robot towards medical applications, IEEE Robot. Automat. Lett. 7 (2022) 5795–5802.)*

4.2.2 Bioadhesive locomotion

The ability to locomote inside organs in vivo is a critical feature necessary for translating magnetic soft robots to minimally invasive surgical applications. This necessitates the robots to move reliably on the surfaces of internal organs (which may be inclined, vertical, or inverted surfaces in confined spaces), working against their own gravity, buoyancy, and friction. Several approaches for improving adhesion have been investigated targeting the aforementioned requirements. Inspired by organisms in nature, special structures and materials have been investigated and verified to have the capability of improving adhesion force on dry or wet condition surfaces [138–140]. For instance, directional mushroom-tipped microfibers inspired by gecko toes have been verified to have strong adhesion and friction on smooth and dry surface [141]. A spider-silk-inspired composite has been reported to have reliable adhesion on wet and cold substrates from 4°C to −196°C [142]. In order to achieve controllable adhesion and detachment for soft robots, an octopus-inspired hydrogel adhesive has been proposed to enhance the stability of robots operation on biological tissues in vitro [143]. Additionally, forces generated by magnetic field gradients have been used to produce tethering forces for adhering soft robots [144].

The surfaces of many animal/human organs such as oral cavity, gastrointestinal tract, and stomach are covered with mucus, where it is intended to provide lubrication and protection for epithelial cells of organ surfaces [145]. Mucus consists primarily of water (95%), making it a highly hydrated system. Due to its lubricating properties, mucus forms a slippery surface which can be difficult for small-scale soft robots to travel over. Film coating on the robot surface can ameliorate interaction properties between the robot and mucus. Chitosan is a widely used polymer because it is able to establish various types of mucus interactions with hydrogen bonds and electrostatic interactions to promote adhesion [146]. Recent work has demonstrated the use of chitosan on a soft robot to provide adhesion to tissue surfaces, with the robot able to carry up to 20 times its own weight. The chitosan is applied to the ends of the robot in combination with microfabricated structures which allows for inchworm-like locomotion [147].

In Ref. [148], a ring-shaped magnetic soft robot, with a flexible biopolymeric film coating, capable of motion on mucus-coated surfaces is designed and investigated. The biopolymeric film made from chitosan-glycerol (C-G) solution endows the robot with robust locomotion capabilities on surfaces of diverse geometrical shapes and orientations. By utilizing mucoadhesive locomotion, the robot has the potential to carry out robotic procedures on enclosed mucus-coated tissue surfaces. In Fig. 14, the robot is shown to perform a pick-and-place operation in a mucus-coated environment. It is also shown that cytotoxicity of the MPC is reduced with the C-G coating, thereby improving the biocompatibility of the robot.

4.2.3 Thermo-magnetic actuation

Thermal triggering under biologically relevant conditions has been increasingly investigated as a remote triggering mechanism for shape change. For example, Leong et al. showed that deformable devices could be actuated even while spatially separated [149]. They demonstrated diverse functions, such as picking up objects in vivo and removing cells from tissue during in vitro biopsies. Liechty et al. proposed drug delivery using polymers that dissolve in a thermally suitable aqueous environment [150].

In the past decade, untethered thermo-magnetic responsive systems have been developed owing to the research of responsive materials such as poly(*N*-isopropyl acrylamide) hydrogels [151] and SMPs [152,153]. These polymers are lightweight and have high strain and shape recovery abilities. SMPs are characterized by their ability to undergo controllable and reversible physical or chemical change under exposure to external stimuli, such as chemicals, light, and magnetic fields [154]. This ability allows for tuning their physical and chemical polymeric properties, including their elasticity, polarity, and strength [155]. Numerous in vivo investigations have been conducted to evaluate the clinical feasibility of magnetic biomedical robotic devices for various applications such as biopsies, pick and place, and drug delivery [156,157]. These devices can be used to retrieve tissue samples from within the body for pathological examination, such as

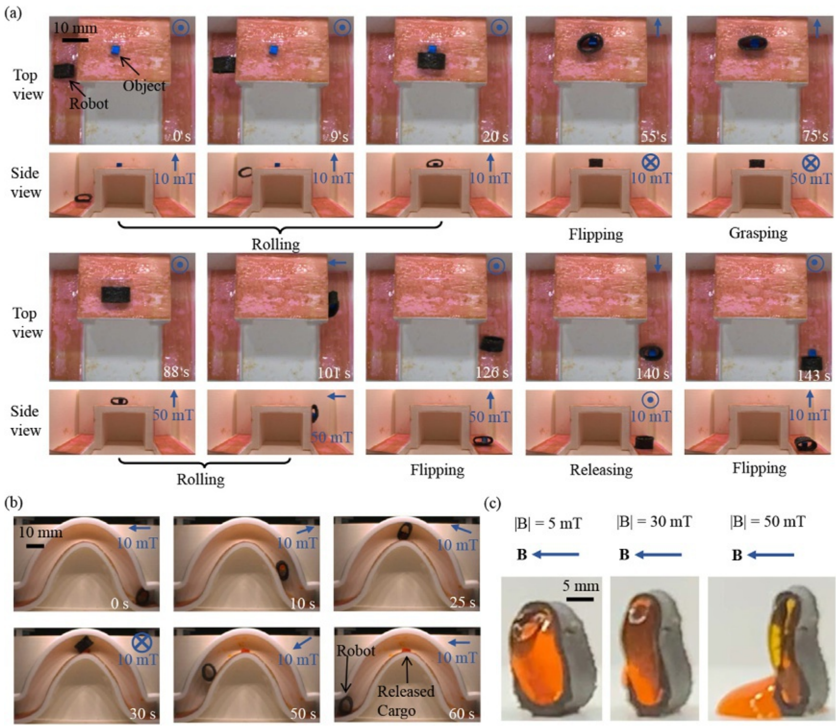

FIG. 14 (A) Experiment to demonstrate the robot performing pick-and-place operation, where the robot moves a target object between two locations at different elevations. Both the top view and side view are shown. The blue arrows represent the directions of the magnetic field at the given time instant. (B) Demonstration of cargo transportation function in a 3D-printed tubular structures. The robot carries a mock-drug up the undulating tube, releases it at the top and subsequently navigates to the bottom. (C) The robot demonstrating carrying of a liquid capsule and compression upon magnetic actuation to expel the liquid. *(Taken from C. Wang, A. Mzyk, R. Schirhagl, S. Misra, V.K. Venkiteswaran, Biocompatible film-coating of magnetic soft robots for mucoadhesive locomotion, Adv. Mater. Technol. (2023) 2201813. https://onlinelibrary.wiley.com/doi/pdf/10.1002/admt.202201813.)*

metallic microgrippers [158] or microdrillers [159]. Additionally, these devices can deliver drugs or other therapeutic agents to a targeted site within the body, including bacterium [160] and microswimmers [161].

In Ref. [162], a magnetically aided thermally triggered shape transformation approach is proposed that leverages the benefits of soft SMPs, bioinspired design, and magnetic actuation. The SMP-based soft carrier only responds to operates at a low temperature for shape transformation. This solution enables its remote actuation, thermal triggering, and drug transport and administration. It is made of a PDMS membrane, a layer of SMP, and a nickel-plated neodymium (NIB) disc magnet (Fig. 15A).

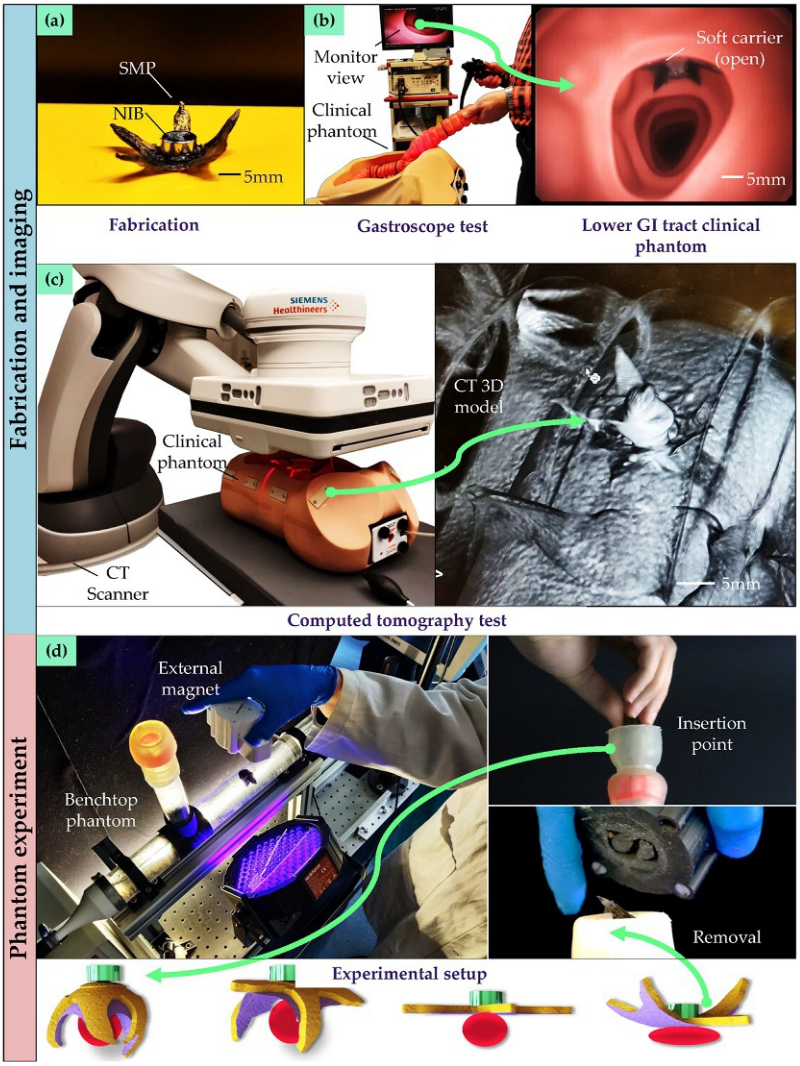

FIG. 15 (A) Fabrication and assembly of the multilayered SMP carrier structure. The soft carrier is then tested within a hybrid operating theatre inside a computed tomography (CT) scanner (Artis Pheno, Siemens Healthineers, Erlangen, Germany), with (B) a gastroscope, and (C) a computed tomography scanner. (D) A benchtop experiment is set up with diameters similar to those of the upper and lower gastrointestinal tracts of the average human adult. The insertion point represents a natural orifice through which the carrier is inserted manually and also retrieved at the end of the experiment. *(Taken from C.M. Heunis, Z. Wang, G. de Vente, S. Misra, V.K. Venkiteswaran, A magnetic bio-inspired soft carrier as a temperature-controlled gastrointestinal drug delivery system, Macromol. Biosci. (2023) 2200559.* https://onlinelibrary.wiley.com/doi/pdf/10.1002/mabi.202200559.)

The carrier is tested for visibility using two imaging modalities. The first is a video gastroscope, which is the conventional tool for routine lower gastrointestinal tract procedures (Fig. 15B). Second, its compatibility within CT images is tested since this method is commonly used to detect internal bleeding (Fig. 15C). The carrier is inserted into a phantom resembling the GI tract at body temperature (Fig. 15D). External fields produced by a permanent magnet influence the guidance and positioning of the carrier and, in addition, enable its subsequent deformation at the target. A gelatin-based biodegradable drug is delivered at a target location. A robust and timely shape recovery performance is achieved, followed by a different shape transformation phase induced by the magnetic field.

4.2.4 Ultrasound-based tracking

Despite developments in the design and actuation of soft robots as described in the previous sections, localization and closed-loop control remain challenges to be solved. A few studies have demonstrated closed-loop control of untethered agents for pick-and-place tasks, using optical camera images [119,163]. However, in many enclosed environments, such as minimally invasive procedures, localization using optical cameras may not be a viable option. Other works have utilized MRI to track and control magnetic untethered robots [164,165]. However, the use of an MR system for the control of soft robots introduces some challenges, such as low control frequency, time delay, and a limited choice of materials for the robot. By contrast, US is an inexpensive and real-time medical imaging modality. Despite the high signal-to-noise ratio, the high frame acquisition rate of US scanning allows real-time control of robots in clinical environments [18,166].

Studies have demonstrated closed-loop control of magnetic robots on the microscale, using US imaging feedback [167,168]. The geometric tracking algorithms employed in these studies are sensitive to noise and to variations in the intensity of the image pixels, and also rely on seeing the same shape of the robot. To increase the robustness of trackers to noise and occlusions, deep learning techniques have been used in computer vision areas for object detection, and regression and classification problems. Convolutional neural networks (CNNs) are often used to estimate the pose of objects in different environments [169]. Additionally, new designs of magnetic soft robots also require sensing of robot orientation to determine the direction of the actuating magnetic field for functions such as cargo delivery, needle biopsy, or maneuvering through the workspace.

de Oliveira et al. [170] demonstrated closed-loop motion control and path planning for a biomimetic magnetic soft robot using 2D US images. A framework is set up for tracking the soft robot and applying the necessary magnetic field for actuation. Two methods for US-based tracking capable of estimating the position and orientation of the robot are investigated, and their performance compared using a video camera as ground truth. Both methods are improvements on trackers in the literature that only estimate the position of microrobots.

Two different approaches are described for the real-time localization of the robot using an US image. The first approach utilizes a geometric algorithm to retrieve the pose of the robot, while the second approach uses a custom-made CNN. The CNN shows a lower error and variance in tracking the soft robot compared to the geometric (RANSAC) method. With the US-based tracking as feedback, closed-loop control is performed in two situations, with an obstacle on one side of the US image, as shown in Fig. 16. In both cases, the robot is able to navigate the obstacles.

However, this study uses a US probe that images a stationary 2D workspace. Furthermore, the size of the image (and thus the workspace) is restricted by the area scanned by the probe. For applications such as the use of soft robots in medical procedures, the US imaging will have to consider motion over greater distances and a dynamic 3D environment with moving obstacles and occlusions.

5. Conclusions

The advent of magnetic actuation in robotics has provided a big fillip to innovations in the field of surgical robotics. Hitherto unprecedented possibilities have been opened up due to the wireless actuation capabilities offered by magnetic fields, along with the benefits offered by rapid temporal response. The human-safe operation with radiation-free power transmission and easy translation to smaller scales mean that this technology is particularly suited to minimally invasive clinical interventions. In this chapter, many works that explore the capabilities offered by this technology are described, ranging from catheters and continuum robots to bioinspired soft robots and US-based tracking. Starting with guiding the tip of a catheter in a blood vessel, studies that propose the use of tether-less multifunctional soft robots within larger organs are presented.

Currently, the maturity of the technology is low, especially considering the stringent safety and reliability standards for medical technology. Existing commercial systems are focused on simple manipulation of magnetic catheters and robotic capsules. One of the key concepts presented in this chapter is that many works rely on using magnetic micro-/nanoparticles, which cause potential bottlenecks with regards to safety during interventions inside the human body. Efforts must be made to overcome this through coating with biocompatible materials or the development of new magneto-responsive components. Another focus area is on developing systems responsive to stimuli that can be used in complement with magnetic actuation (e.g., thermal, chemical) to endow the systems with additional actuation degrees of freedom. Methods to track and reliably maneuver magnetic devices are also still lacking, particularly in the clinical context. Ultimately, developments in this field must take into account existing clinical infrastructure and their constraints, as well as established medical protocols. Future works should incorporate input from medical professionals to

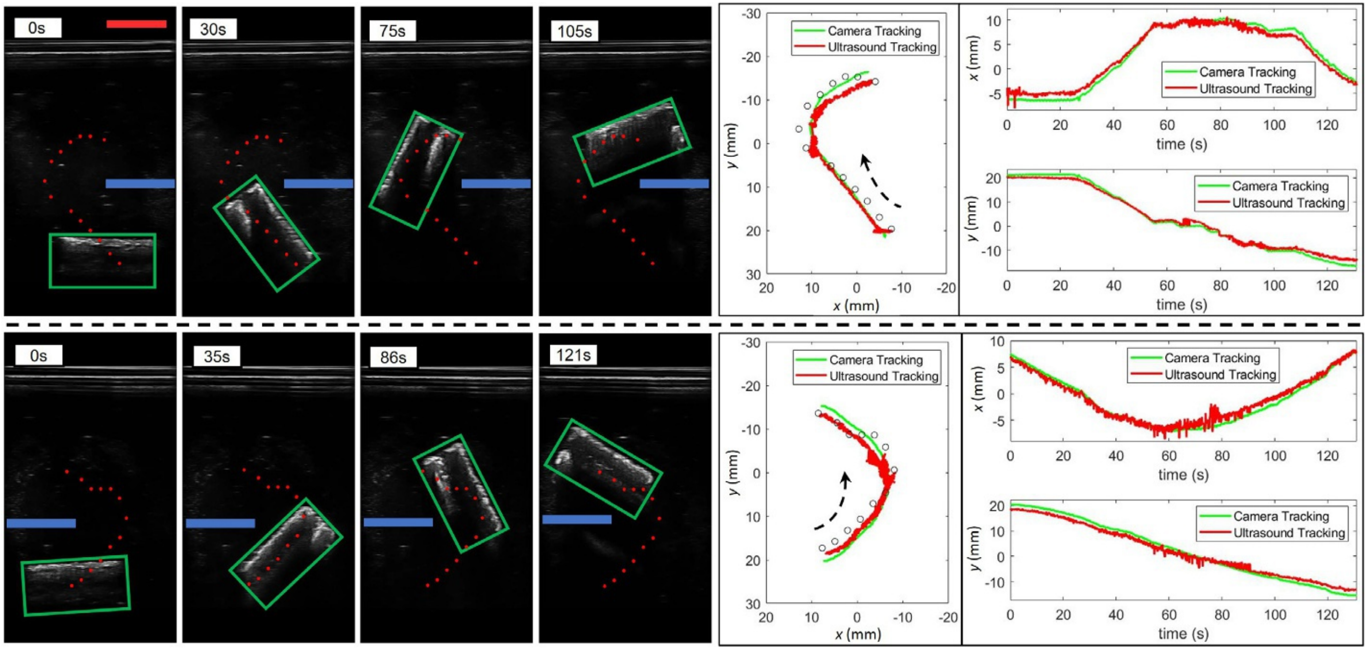

FIG. 16 Closed-loop control of a soft robot using a convolutional neural network (CNN) to detect the pose of the robot in US images. The experiment shows the steering of the Millipede robot to a target while avoiding an obstacle on the right (top column) and on the left side (bottom column). The scale bar is 20 mm. Plots on the right show the comparison of the trajectory obtained using the CNN tracker and the camera tracker (ground truth). *(Taken from A.J.A. de Oliveira, J. Batista, S. Misra, V.K. Venkiteswaran, Ultrasound tracking and closed-loop control of a magnetically-actuated biomimetic soft robot, in: 2022 IEEE/RSJ International Conference on Intelligent Robots and Systems (IROS), 2022, pp. 3422–3428, ISSN: 2153-0866.)*

ensure the promise of the technology can be translated successfully into better outcomes for health providers and patients.

Acknowledgments

This work was supported by the European Research Council (ERC) under the European Union's Horizon 2020 Research and Innovation program under grant 866494 project—MAESTRO.

This chapter is based on results from multiple research projects at Surgical Robotics Laboratory, at University of Twente and University Medical Centre Groningen, the Netherlands. The authors would like to acknowledge the efforts of the individual researchers who were involved in these projects: Artur Anjos de Oliviera, Gerko de Vente, Luis Pena Fernando Samaniego, Juan Huarato Sevilla, Christoff Heunis, Mert Kaya, Venkata Rithwick Puranam, Michiel Richter, Jakub Sikorski, Danica Tan, Theodosia Thomas, and Chen Wang. The authors would also like to acknowledge the input from collaborators: Prof. Leon Abelmann, Prof. G. K. Ananthasuresh, Prof. Jorge Batista, Dr. Aldona Myzk, and Prof. Romana Schirhagl.

References

[1] P.L. Gildenberg, The history of stereotactic neurosurgery, Neurosurg. Clin. N. Am. 1 (1990) 765–780.

[2] Y. Kwoh, J. Hou, E. Jonckheere, S. Hayati, A robot with improved absolute positioning accuracy for CT guided stereotactic brain surgery, IEEE Trans. Biomed. Eng. 35 (1988) 153–160.

[3] S.J. Harris, F. Arambula-Cosio, Q. Mei, R.D. Hibberd, B.L. Davies, J.E.A. Wickham, M.S. Nathan, B. Kundu, The Probot—an active robot for prostate resection, Proc. Inst. Mech. Eng. H: J. Eng. Med. 211 (1997) 317–325.

[4] G. Ballantyne, Robotic surgery, telerobotic surgery, telepresence, and telementoring, Surg. Endosc. Other Interv. Tech. 16 (2002) 1389–1402.

[5] N.G. Hockstein, C.G. Gourin, R.A. Faust, D.J. Terris, A history of robots: from science fiction to surgical robotics, J. Robot. Surg. 1 (2007) 113–118.

[6] C. Bergeles, G.-Z. Yang, From passive tool holders to microsurgeons: safer, smaller, smarter surgical robots, IEEE Trans. Biomed. Eng. 61 (2014) 1565–1576.

[7] G. Robinson, J. Davies, Continuum robots—a state of the art, in: Proceedings 1999 IEEE International Conference on Robotics and Automation (Cat. No. 99CH36288C), vol. 4, 1999, pp. 2849–2854.

[8] V.K. Venkiteswaran, J. Sikorski, S. Misra, Shape and contact force estimation of continuum manipulators using pseudo rigid body models, Mech. Mach. Theory 139 (2019) 34–45.

[9] J. Burgner-Kahrs, D.C. Rucker, H. Choset, Continuum robots for medical applications: a survey, IEEE Trans. Robot. 31 (2015) 1261–1280.

[10] M. Tonutti, D.S. Elson, G.Z. Yang, A.W. Darzi, M.H. Sodergren, The role of technology in minimally invasive surgery: state of the art, recent developments and future directions, Postgrad. Med. J. 93 (1097) (2017) 159–167.

[11] M. Eshaghi, M. Ghasemi, K. Khorshidi, Design, manufacturing and applications of small-scale magnetic soft robots, Extreme Mech. Lett. (2021) 101268.

[12] D. Rus, M.T. Tolley, Design, fabrication and control of soft robots, Nature 521 (7553) (2015) 467–475.

[13] D.J. Griffiths, Introduction to Electrodynamics, Prentice Hall, 1999.

[14] A.J. Petruska, B.J. Nelson, Minimum bounds on the number of electromagnets required for remote magnetic manipulation, IEEE Trans. Robot. 31 (3) (2015) 714–722.
[15] A.J. Petruska, J.J. Abbott, Optimal permanent-magnet geometries for dipole field approximation, IEEE Trans. Magn. 49 (2) (2012) 811–819.
[16] M.P. Kummer, J.J. Abbott, B.E. Kratochvil, R. Borer, A. Sengul, B.J. Nelson, Octomag: an electromagnetic system for 5-dof wireless micromanipulation, IEEE Trans. Robot. 26 (6) (2010) 1006–1017.
[17] M. Sitti, H. Ceylan, W. Hu, J. Giltinan, M. Turan, S. Yim, E. Diller, Biomedical applications of untethered mobile milli/microrobots, Proc. IEEE 103 (2015) 205–224.
[18] B.J. Nelson, I.K. Kaliakatsos, J.J. Abbott, Microrobots for minimally invasive medicine, Annu. Rev. Biomed. Eng. 12 (2010) 55–85.
[19] F. Ongaro, S. Scheggi, A. Ghosh, A. Denasi, D.H. Gracias, S. Misra, Design, characterization and control of thermally-responsive and magnetically-actuated micro-grippers at the air-water interface, PLoS One 12 (12) (2017) e0187441.
[20] G. Pittiglio, L. Barducci, J.W. Martin, J.C. Norton, C.A. Avizzano, K.L. Obstein, P. Valdastri, Magnetic levitation for soft-tethered capsule colonoscopy actuated with a single permanent magnet: a dynamic control approach, IEEE Robot. Automat. Lett. 4 (2) (2019) 1224–1231.
[21] H. Tillander, Magnetic guidance of a catheter with articulated steel tip, Acta Radiol. 35 (1) (1951) 62–64.
[22] C.M. Heunis, Y.P. Wotte, J. Sikorski, et al., The armm system-autonomous steering of magnetically-actuated catheters: towards endovascular applications, IEEE Robot. Autom. Lett. 5 (2) (2020) 705–712.
[23] J. Edelmann, A.J. Petruska, B.J. Nelson, Magnetic control of continuum devices, Int. J. Robot. Res. 36 (1) (2017) 68–85.
[24] C. Chautems, S. Lyttle, Q. Boehler, B.J. Nelson, Design and evaluation of a steerable magnetic sheath for cardiac ablations, IEEE Robot. Automat. Lett. 3 (3) (2018) 2123–2128.
[25] A.D. Losey, P. Lillaney, A.J. Martin, et al., Magnetically assisted remote-controlled endovascular catheter for interventional MR imaging: in vitro navigation at 1.5 T versus x-ray fluoroscopy, Radiology 271 (3) (2014) 862–869.
[26] F. Carpi, C. Pappone, Stereotaxis niobe® magnetic navigation system for endocardial catheter ablation and gastrointestinal capsule endoscopy, Expert Rev. Med. Devices 6 (5) (2009) 487–498.
[27] S.A. Virk, S. Kumar, Remote magnetic versus manual catheter navigation for atrial fibrillation ablation: a meta-analysis, Circ. Arrhythm. Electrophysiol. 12 (10) (2019) e007517.
[28] L. Lüthje, D. Vollmann, J. Seegers, M. Dorenkamp, C. Sohns, G. Hasenfuss, M. Zabel, Remote magnetic versus manual catheter navigation for circumferential pulmonary vein ablation in patients with atrial fibrillation, Clin. Res. Cardiol. 100 (2011) 1003–1011.
[29] R. Proietti, V. Pecoraro, L. Di Biase, A. Natale, P. Santangeli, M. Viecca, A. Sagone, A. Galli, L. Moja, L. Tagliabue, Remote magnetic with open-irrigated catheter vs. manual navigation for ablation of atrial fibrillation: a systematic review and meta-analysis, Europace 15 (9) (2013) 1241–1248.
[30] S. Salmanipour, E. Diller, Eight-degrees-of-freedom remote actuation of small magnetic mechanisms, in: IEEE International Conference on Robotics and Automation (ICRA), 2018.
[31] J. Sikorski, I. Dawson, A. Denasi, E.E. Hekman, S. Misra, Introducing BigMag—A Novel System for 3d Magnetic Actuation of Flexible Surgical Manipulators, IEEE, 2017, pp. 3594–3599.

[32] J. Sikorski, C.M. Heunis, F. Franco, S. Misra, The armm system: an optimized mobile electromagnetic coil for non-linear actuation of flexible surgical instruments, IEEE Trans. Magn. 55 (9) (2019) 1–9.
[33] C.M. Heunis, J. Sikorski, S. Misra, Flexible instruments for endovascular interventions: improved magnetic steering, actuation, and image-guided surgical instruments, IEEE Robo. Automat. Mag. 25 (3) (2018) 71–82.
[34] F. Ongaro, C.M. Heunis, S. Misra, Precise model-free spline-based approach for magnetic field mapping, IEEE Magn. Lett. 10 (2018) 1–5.
[35] A.J. Petruska, J. Edelmann, B.J. Nelson, Model-based calibration for magnetic manipulation, IEEE Trans. Magn. 53 (7) (2017) 1–6.
[36] M. Richter, V.K. Venkiteswaran, S. Misra, Multi-point orientation control of discretely-magnetized continuum manipulators, IEEE Robot. Autom. Lett. 6 (2) (2021) 3607–3614.
[37] G.S. Chirikjian, J.W. Burdick, A hyper-redundant manipulator, IEEE Robo. Automat. Mag. 1 (4) (1994) 22–29.
[38] V. Vitiello, S.-L. Lee, T.P. Cundy, G.-Z. Yang, Emerging robotic platforms for minimally invasive surgery, IEEE Rev. Biomed. Eng. 6 (2012) 111–126.
[39] C. Bergeles, G.-Z. Yang, From passive tool holders to microsurgeons: safer, smaller, smarter surgical robots, IEEE Trans. Biomed. Eng. 61 (5) (2013) 1565–1576.
[40] C. Pappone, G. Vicedomini, F. Manguso, F. Gugliotta, P. Mazzone, S. Gulletta, N. Sora, S. Sala, A. Marzi, G. Augello, L. Livolsi, A Santagostino, V. Santinelli, Robotic magnetic navigation for atrial fibrillation ablation, J. Am. Coll. Cardiol. 47 (7) (2006) 1390–1400, https://doi.org/10.1016/j.jacc.2005.11.058. Epub 2006 Mar 15.
[41] L.B. Kratchman, T.L. Bruns, J.J. Abbott, R.J. Webster, Guiding elastic rods with a robot-manipulated magnet for medical applications, IEEE Trans. Robot. 33 (1) (2016) 227–233.
[42] T. da Veiga, J.H. Chandler, P. Lloyd, G. Pittiglio, N.J. Wilkinson, A.K. Hoshiar, R.A. Harris, P. Valdastri, Challenges of continuum robots in clinical context: a review, Progr. Biomed. Eng. (2020).
[43] J. Sikorski, S. Mohanty, S. Misra, Milimac: flexible catheter with miniaturized electromagnets as a small-footprint system for microrobotic tasks, IEEE Robot. Automat. Lett. 5 (4) (2020) 5260–5267.
[44] Y. Kim, G.A. Parada, S. Liu, X. Zhao, Ferromagnetic soft continuum robots, Sci. Robot. 4 (33) (2019) 7329.
[45] P. Lloyd, A.K. Hoshiar, T. da Veiga, A. Attanasio, N. Marahrens, J.H. Chandler, P. Valdastri, A learnt approach for the design of magnetically actuated shape forming soft tentacle robots, IEEE Robot. Automat. Lett. 5 (3) (2020) 3937–3944.
[46] G.Z. Lum, Z. Ye, X. Dong, H. Marvi, O. Erin, W. Hu, M. Sitti, Shape-programmable magnetic soft matter, Proc. Natl. Acad. Sci. 113 (41) (2016) E6007–E6015.
[47] A. Ali, A. Sakes, E.A. Arkenbout, et al., Catheter steering in interventional cardiology: mechanical analysis and novel solution, Proc. Inst. Mech. Eng. H 233 (12) (2019) 1207–1218.
[48] K.H. Polderman, A.R. Girbes, Central venous catheter use. Part 1. Mechanical complications, Intensive Care Med. 28 (2002) 1–17.
[49] F.K. Wacker, J. Boese-Landgraf, A. Wagner, D. Albrecht, K.-J. Wolf, F. Fobbe, Minimally invasive catheter implantation for regional chemotherapy of the liver: a new percutaneous transsubclavian approach, Cardiovasc. Intervent. Radiol. 20 (1997) 128–132.
[50] R. Roelz, V.A. Coenen, C. Scheiwe, W.-D. Niesen, K. Egger, I. Csok, R. Kraeutle, R. Jabbarli, H. Urbach, P.C. Reinacher, Stereotactic catheter ventriculocisternostomy for clearance of subarachnoid hemorrhage: a matched cohort study, Stroke 48 (10) (2017) 2704–2709.

[51] O.C. Mora, P. Zanne, L. Zorn, F. Nageotte, N. Zulina, S. Gravelyn, P. Montgomery, M. De Mathelin, B. Dallemagne, M.J. Gora, Steerable oct catheter for real-time assistance during teleoperated endoscopic treatment of colorectal cancer, Biomed. Opt. Express 11 (3) (2020) 1231–1243.

[52] R. Cappato, H. Calkins, S.-A. Chen, W. Davies, Y. Iesaka, J. Kalman, Y.-H. Kim, G. Klein, D. Packer, A. Skanes, Worldwide survey on the methods, efficacy, and safety of catheter ablation for human atrial fibrillation, Circulation 111 (9) (2005) 1100–1105.

[53] G.A. Antoniou, C.V. Riga, E.K. Mayer, N.J. Cheshire, C.D. Bicknell, Clinical applications of robotic technology in vascular and endovascular surgery, J. Vasc. Surg. 53 (2) (2011) 493–499.

[54] H. Rafii-Tari, C.J. Payne, G.-Z. Yang, Current and emerging robot-assisted endovascular catheterization technologies: a review, Ann. Biomed. Eng. 42 (2014) 697–715.

[55] S.A. Menaker, S.S. Shah, B.M. Snelling, S. Sur, R.M. Starke, E.C. Peterson, Current applications and future perspectives of robotics in cerebrovascular and endovascular neurosurgery, J. Neurointervent. Surg. 10 (1) (2018) 78–82.

[56] S.L. Charreyron, Q. Boehler, A.N. Danun, et al., A magnetically navigated microcannula for subretinal injections, IEEE Trans. Biomed. Eng. 68 (1) (2020) 119–129.

[57] S. Jeon, A.K. Hoshiar, K. Kim, S. Lee, E. Kim, S. Lee, J.-Y. Kim, B.J. Nelson, H.-J. Cha, B.-J. Yi, H. Choi, A magnetically controlled soft microrobot steering a guidewire in a three-dimensional phantom vascular network, Soft Robot. (2018).

[58] P.R. Slawinski, A.Z. Taddese, K.B. Musto, K.L. Obstein, P. Valdastri, Autonomous retroflexion of a magnetic flexible endoscope, IEEE Robot. Automat. Lett. 2 (3) (2017) 1352–1359.

[59] J.H. Chandler, M. Chauhan, N. Garbin, K.L. Obstein, P. Valdastri, Parallel helix actuators for soft robotic applications, Front. Robot. AI 7 (2020) 119.

[60] K.M. Popek, T. Hermans, J.J. Abbott, First demonstration of simultaneous localization and propulsion of a magnetic capsule in a lumen using a single rotating magnet, in: 2017 IEEE International Conference on Robotics and Automation (ICRA), IEEE, 2017, pp. 1154–1160.

[61] C. Chautems, B.J. Nelson, The tethered magnet: Force and 5-DOF pose control for cardiac ablation, in: IEEE International Conference on Robotics and Automation, 2017, pp. 4837–4842.

[62] D. Son, H. Gilbert, M. Sitti, Magnetically actuated soft capsule endoscope for fine-needle biopsy, Soft Robot. 7 (1) (2020) 10–21.

[63] S. Jeon, A.K. Hoshiar, K. Kim, S. Lee, E. Kim, S. Lee, J.-Y. Kim, B.J. Nelson, H.-J. Cha, B.-J. Yi, et al., A magnetically controlled soft microrobot steering a guidewire in a three-dimensional phantom vascular network, Soft Robot. 6 (1) (2019) 54–68.

[64] V.K. Venkiteswaran, L.F.P. Samaniego, J. Sikorski, S. Misra, Bio-inspired terrestrial motion of magnetic soft millirobots, IEEE Robot. Automat. Lett. 4 (2019) 1753–1759.

[65] E. Diller, J. Zhuang, G. Zhan Lum, M.R. Edwards, M. Sitti, Continuously distributed magnetization profile for millimeter-scale elastomeric undulatory swimming, Appl. Phys. Lett. 104 (2014) 174101.

[66] H. Lu, M. Zhang, Y. Yang, Q. Huang, T. Fukuda, Z. Wang, Y. Shen, A bioinspired multilegged soft millirobot that functions in both dry and wet conditions, Nat. Commun. 9 (2018) 3944.

[67] P.J. Swaney, J. Burgner, H.B. Gilbert, R.J. Webster, A flexure-based steerable needle: high curvature with reduced tissue damage, IEEE Trans. Biomed. Eng. 60 (4) (2012) 906–909.

[68] K. Chandrasekaran, A. Sathuluri, A. Thondiyath, Magnex—expendable robotic surgical tool-tip, in: 2017 IEEE International Conference on Robotics and Automation (ICRA), IEEE, 2017, pp. 4221–4226.

[69] K. Chandrasekaran, A. Thondiyath, Design of a two degree-of-freedom compliant tool tip for a handheld powered surgical tool, J. Med. Dev. 11 (1) (2017).

[70] Y.-J. Kim, S. Cheng, S. Kim, K. Iagnemma, Design of a tubular snake-like manipulator with stiffening capability by layer jamming, in: 2012 IEEE/RSJ International Conference on Intelligent Robots and Systems, IEEE, 2012, pp. 4251–4256.

[71] T. Kato, I. Okumura, S.-E. Song, A.J. Golby, N. Hata, Tendon-driven continuum robot for endoscopic surgery: preclinical development and validation of a tension propagation model, IEEE/ASME Trans. Mechatron. 20 (5) (2014) 2252–2263.

[72] W. Saliba, J.E. Cummings, S. Oh, Y. Zhang, T.N. Mazgalev, R.A. Schweikert, J.D. Burkhardt, A. Natale, Novel robotic catheter remote control system: feasibility and safety of transseptal puncture and endocardial catheter navigation, J. Cardiovasc. Electrophysiol. 17 (10) (2006) 1102–1105.

[73] T.L. Thomas, V.K. Venkiteswaran, G.K. Ananthasuresh, S. Misra, A monolithic compliant continuum manipulator: a proof-of-concept study, J. Mech. Robot. 12 (2020).

[74] T.L. Thomas, J. Sikorski, G. Ananthasuresh, V.K. Venkiteswaran, S. Misra, Design, sensing, and control of a magnetic compliant continuum manipulator, IEEE Trans. Med. Robot. Bionics (2022) 1.

[75] J. Zhang, Z. Ren, W. Hu, R.H. Soon, I.C. Yasa, Z. Liu, M. Sitti, Voxelated three-dimensional miniature magnetic soft machines via multimaterial heterogeneous assembly, Sci. Robot. 6 (53) (2021).

[76] Y. Kim, H. Yuk, R. Zhao, et al., Printing ferromagnetic domains for untethered fast-transforming soft materials, Nature 558 (7709) (2018) 274–279.

[77] S. Wu, W. Hu, Q. Ze, M. Sitti, R. Zhao, Multifunctional magnetic soft composites: a review, Multifunct. Mater. 3 (4) (2020) 042003.

[78] Y. Kim, X. Zhao, Magnetic soft materials and robots, Chem. Rev. 122 (5) (2022) 5317–5364.

[79] L. Wang, D. Zheng, P. Harker, et al., Evolutionary design of magnetic soft continuum robots, Proc. Natl. Acad. Sci. 118 (21) (2021).

[80] C. Chautems, A. Tonazzini, Q. Boehler, S.H. Jeong, D. Floreano, B.J. Nelson, Magnetic continuum device with variable stiffness for minimally invasive surgery, Adv. Intell. Syst. 2 (6) (2020) 1900086.

[81] F.P. Gosselin, V. Lalande, S. Martel, Characterization of the deflections of a catheter steered using a magnetic resonance imaging system, Med. Phys. 38 (9) (2011) 4994–5002.

[82] M. Richter, M. Kaya, J. Sikorski, L. Abelmann, V. Kalpathy Venkiteswaran, S. Misra, Magnetic soft helical manipulators with local dipole interactions for flexibility and forces, Soft Robot. (2023).

[83] J. Hwang, S. Jeon, B. Kim, et al., An electromagnetically controllable microrobotic interventional system for targeted, real-time cardiovascular intervention, Adv Healthc Mater 11 (11) (2022) 2102529.

[84] W. Dou, G. Zhong, J. Cao, Z. Shi, B. Peng, L. Jiang, Soft robotic manipulators: designs, actuation, stiffness tuning, and sensing, Adv. Mater. Technol. 6 (9) (2021) 2100018.

[85] M. Brancadoro, M. Manti, F. Grani, S. Tognarelli, A. Menciassi, M. Cianchetti, Toward a variable stiffness surgical manipulator based on fiber jamming transition, Front. Robot. AI 6 (2019) 12.

[86] D.S. Shah, E.J. Yang, M.C. Yuen, E.C. Huang, R. Kramer-Bottiglio, Jamming skins that control system rigidity from the surface, Adv. Funct. Mater. 31 (1) (2021) 2006915.

[87] K. Althoefer, Antagonistic actuation and stiffness control in soft inflatable robots, Nat. Rev. Mater. 3 (6) (2018) 76–77.

[88] M.E. Giannaccini, C. Xiang, A. Atyabi, T. Theodoridis, S. Nefti-Meziani, S. Davis, Novel design of a soft lightweight pneumatic continuum robot arm with decoupled variable stiffness and positioning, Soft Robot. 5 (2018) 54–70.
[89] J. Zhu, L. Lyu, Y. Xu, H. Liang, X. Zhang, H. Ding, Z. Wu, Intelligent soft surgical robots for next-generation minimally invasive surgery, Adv. Intell. Syst. 3 (5) (2021) 2100011.
[90] Y. Zhong, L. Hu, Y. Xu, Recent advances in design and actuation of continuum robots for medical applications, in: Actuators, vol. 9, MDPI, 2020, p. 142.
[91] F. Alambeigi, R. Seifabadi, M. Armand, A continuum manipulator with phase changing alloy, in: 2016 IEEE International Conference on Robotics and Automation (ICRA), IEEE, 2016, pp. 758–764.
[92] C. Yang, S. Geng, I. Walker, D.T. Branson, J. Liu, J.S. Dai, R. Kang, Geometric constraint-based modeling and analysis of a novel continuum robot with shape memory alloy initiated variable stiffness, Int. J. Robot. Res. 39 (14) (2020) 1620–1634.
[93] M. Mattmann, C. De Marco, F. Briatico, S. Tagliabue, A. Colusso, X.-Z. Chen, J. Lussi, C. Chautems, S. Pané, B. Nelson, Thermoset shape memory polymer variable stiffness 4d robotic catheters, Adv. Sci. 9 (1) (2022) 2103277.
[94] J. Lussi, M. Mattmann, S. Sevim, F. Grigis, C. De Marco, C. Chautems, S. Pané, J. Puigmartí-Luis, Q. Boehler, B.J. Nelson, A submillimeter continuous variable stiffness catheter for compliance control, Adv. Sci. 8 (18) (2021) 2101290.
[95] H. Jeon, Q.N. Le, S. Jeong, S. Jang, H. Jung, H. Chang, H.J. Pandya, Y. Kim, Towards a snake-like flexible robot with variable stiffness using an sma spring-based friction change mechanism, IEEE Robot. Automat. Lett. 7 (3) (2022) 6582–6589.
[96] Y. Cao, F. Ju, L. Zhang, D. Bai, F. Qi, B. Chen, A novel variable-stiffness flexible manipulator actuated by shape memory alloy for minimally invasive surgery, Proc. Inst. Mech. Eng. H J. Eng. Med. 232 (11) (2018) 1098–1110.
[97] S. Jiang, B. Chen, F. Qi, Y. Cao, F. Ju, D. Bai, Y. Wang, A variable-stiffness continuum manipulators by an sma-based sheath in minimally invasive surgery, Int. J. Med. Robot. Comput. Assist. Surg. 16 (2) (2020) e2081.
[98] M.C. Yuen, R.A. Bilodeau, R.K. Kramer, Active variable stiffness fibers for multifunctional robotic fabrics, IEEE Robot. Automat. Lett. 1 (2) (2016) 708–715.
[99] A. Lendlein, O.E. Gould, Reprogrammable recovery and actuation behaviour of shape-memory polymers, Nat. Rev. Mater. 4 (2) (2019) 116–133.
[100] K. Wang, Y.-G. Jia, C. Zhao, X. Zhu, Multiple and two-way reversible shape memory polymers: Design strategies and applications, Prog. Mater. Sci. 105 (2019) 100572.
[101] Y. Piskarev, J. Shintake, C. Chautems, J. Lussi, Q. Boehler, B.J. Nelson, D. Floreano, A variable stiffness magnetic catheter made of a conductive phase-change polymer for minimally invasive surgery, Adv. Funct. Mater. (2022) 2107662.
[102] T.L. Thomas, J. Bos, J.J. Huaroto, V. Kalpathy Venkiteswaran, S. Misra, A magnetically actuated variable stiffness manipulator based on deployable shape memory polymer springs, Adv. Intell. Syst. (2023) 2200465. https://onlinelibrary.wiley.com/doi/pdf/10.1002/aisy.202200465.
[103] S. Ernst, F. Ouyang, C. Linder, K. Hertting, F. Stahl, J. Chun, H. Hachiya, D. Bansch, M. Antz, K. Kuck, Initial experience with remote catheter ablation using a novel magnetic navigation system: magnetic remote catheter ablation, Circulation 109 (12) (2004) 1472–1475.
[104] T. Gildea, P. Mazzone, D. Karnak, M. Meziane, A. Mehta, Electromagnetic navigation diagnostic bronchoscopy: a prospective study, Am. J. Respir. Crit. Care Med. 174 (9) (2006) 982–989.

[105] J. Kim, S.E. Chung, S.-E. Choi, H. Lee, J. Kim, S. Kwon, Programming magnetic anisotropy in polymeric microactuators, Nat. Mater. 10 (2011) nmat3090.
[106] V.Q. Nguyen, A.S. Ahmed, R.V. Ramanujan, Morphing soft magnetic composites, Adv. Mater. 24 (2012) 4041–4054.
[107] P. Garstecki, P. Tierno, D.B. Weibel, F. Sagues, G.M. Whitesides, Propulsion of flexible polymer structures in a rotating magnetic field, J. Phys. Condens. Matter 21 (20) (2009).
[108] W. Hu, G.Z. Lum, M. Mastrangeli, M. Sitti, Small-scale soft-bodied robot with multimodal locomotion, Nature 554 (2018) 81–85.
[109] J. Zhang, E. Diller, Untethered miniature soft robots: modeling and design of a millimeter-scale swimming magnetic sheet, Soft Robot. (2018).
[110] J.B. Mathieu, S. Martel, L. Yahia, G. Soulez, G. Beaudoin, Preliminary studies for using magnetic resonance imaging systems as a mean of propulsion for microrobots in blood vessels and evaluation of ferromagnetic artefacts, in: CCECE 2003—Canadian Conference on Electrical and Computer Engineering. Toward a Caring and Humane Technology (Cat. No.03CH37436), vol. 2, 2003, pp. 835–838.
[111] A. Azizi, C.C. Tremblay, K. Gagné, S. Martel, Using the fringe field of a clinical MRI scanner enables robotic navigation of tethered instruments in deeper vascular regions, Sci. Robot. 4 (2019).
[112] T. Xu, J. Zhang, M. Salehizadeh, O. Onaizah, E. Diller, Millimeter-scale flexible robots with programmable three-dimensional magnetization and motions, Sci. Robot. 4 (2019) eaav4494.
[113] C. Pacchierotti, F. Ongaro, F. van den Brink, C. Yoon, D. Prattichizzo, D.H. Gracias, S. Misra, Steering and control of miniaturized untethered soft magnetic grippers with haptic assistance, IEEE Trans. Autom. Sci. Eng. 15 (2018) 290–306.
[114] A. Ghosh, C. Yoon, F. Ongaro, S. Scheggi, F.M. Selaru, S. Misra, D.H. Gracias, Stimuli-responsive soft untethered grippers for drug delivery and robotic surgery, Front. Mech. Eng. 3 (2017).
[115] S. Fusco, M.S. Sakar, S. Kennedy, C. Peters, S. Pane, D. Mooney, B.J. Nelson, Self-folding mobile microrobots for biomedical applications, in: 2014 IEEE International Conference on Robotics and Automation (ICRA), 2014, pp. 3777–3782.
[116] E. Diller, M. Sitti, Three-dimensional programmable assembly by untethered magnetic robotic micro-grippers, Adv. Funct. Mater. 24 (28) (2014) 4397–4404.
[117] M.P.D. Cunha, Y. Foelen, R.J.H.V. Raak, J.N. Murphy, T.A.P. Engels, M.G. Debije, A.P.H.J. Schenning, An untethered magnetic- and light-responsive rotary gripper: shedding light on photoresponsive liquid crystal actuators, Adv. Opt. Mater. 7 (7) (2019) 1801643.
[118] S.E. Chung, X. Dong, M. Sitti, Three-dimensional heterogeneous assembly of coded microgels using an untethered mobile microgripper, Lab Chip 15 (2015) 1667–1676.
[119] J. Zhang, O. Onaizah, K. Middleton, L. You, E. Diller, Reliable grasping of three-dimensional untethered mobile magnetic microgripper for autonomous pick-and-place, IEEE Robot. Automat. Lett. 2 (2) (2017) 835–840.
[120] K.-J. Cho, R. Wood, Biomimetic robots, in: B. Siciliano, O. Khatib (Eds.), Springer Handbook of Robotics, Springer International Publishing, Cham, 2016, pp. 543–574.
[121] U. Saranli, M. Buehler, D.E. Koditschek, RHex: a simple and highly mobile hexapod robot, Int. J. Robot. Res. 20 (2001) 616–631.
[122] C. Li, T. Zhang, D.I. Goldman, A terradynamics of legged locomotion on granular media, Science 339 (2013) 1408–1412.
[123] R. Wood, The first takeoff of a biologically inspired at-scale robotic insect, IEEE Trans. Robot. 24 (2) (2008) 341–347.

[124] M. Keennon, K. Klingebiel, H. Won, A. Andriukov, Development of the Nano Hummingbird: A Tailless Flapping Wing Micro Air Vehicle, in: 50th AIAA Aerospace Sciences Meeting including the New Horizons Forum and Aerospace Exposition (Nashville, Tennessee), 2012, p. 588.

[125] S. Kim, M. Spenko, S. Trujillo, B. Heyneman, D. Santos, M.R. Cutkosky, Smooth vertical surface climbing with directional adhesion, IEEE Trans. Robot. 24 (2008) 65–74.

[126] J. Sikorski, I. Dawson, A. Denasi, E.E.G. Hekman, S. Misra, Introducing BigMag - A novel system for 3d magnetic actuation of flexible surgical manipulators, in: 2017 IEEE International Conference on Robotics and Automation (ICRA), 2017, pp. 3594–3599.

[127] V.K. Venkiteswaran, D.K. Tan, S. Misra, Tandem actuation of legged locomotion and grasping manipulation in soft robots using magnetic fields, Extreme Mech. Lett. 93 (1097) (2017).

[128] M. Golubitsky, I. Stewart, P.-L. Buono, J.J. Collins, Symmetry in locomotor central pattern generators and animal gaits, Nature 401 (1999) 693–695.

[129] T. Lee, C. Liao, T.K. Chen, On the stability properties of hexapod tripod gait, IEEE J. Robot. Automat. 4 (1988) 427–434.

[130] P. Birkmeyer, K. Peterson, R.S. Fearing, DASH: A dynamic 16g hexapedal robot, in: 2009 IEEE/RSJ International Conference on Intelligent Robots and Systems, 2009, pp. 2683–2689.

[131] S.R. Goudu, I.C. Yasa, X. Hu, H. Ceylan, W. Hu, M. Sitti, Biodegradable untethered magnetic hydrogel milli-grippers, Adv. Funct. Mater. 30 (50) (2020) 2004975.

[132] U. Bozuyuk, O. Yasa, I. Yasa, H. Ceylan, S. Kizilel, M. Sitti, Light-triggered drug release from 3d-printed magnetic chitosan microswimmers, ACS Nano 12 (9) (2018) 9617–9625.

[133] H. Ceylan, I.C. Yasa, O. Yasa, A.F. Tabak, J. Giltinan, M. Sitti, 3d-printed biodegradable microswimmer for theranostic cargo delivery and release, ACS Nano 13 (3) (2019) 3353–3362.

[134] M. Baumgartner, F. Hartmann, M. Drack, D. Preninger, D. Wirthl, R. Gerstmayr, L. Lehner, G. Mao, R. Pruckner, S. Demchyshyn, L. Reiter, Resilient yet entirely degradable gelatin-based biogels for soft robots and electronics, Nat. Mater. 19 (10) (2020) 1102–1109.

[135] S. Miyashita, S. Guitron, K. Yoshida, S. Li, D. Damian, D. Rus, Ingestible, controllable, and degradable origami robot for patching stomach wounds, in: Proceedings of International Conference on Robotics and Automation, 2016, pp. 909–916.

[136] J. Hughes, D. Rus, Mechanically programmable, degradable & ingestible soft actuators, in: Proceedings of IEEE International Conference on Soft Robotics, 2020, pp. 836–843.

[137] C. Wang, V.R. Puranam, S. Misra, V.K. Venkiteswaran, A snake-inspired multi-segmented magnetic soft robot towards medical applications, IEEE Robot. Automat. Lett. 7 (2022) 5795–5802.

[138] X. Zhang, G. Chen, Y. Yu, L. Sun, Y. Zhao, Bioinspired adhesive and antibacterial microneedles for versatile transdermal drug delivery, Research (2020).

[139] M. Baby, V.K. Periya, S.K. Sankaranarayanan, S.C. Maniyeri, Bioinspired surface activators for wet/dry environments through greener epoxy-catechol amine chemistry, Appl. Surf. Sci. 505 (2020).

[140] X.-C. Li, D.-Z. Hao, W.-J. Hao, X.-L. Guo, L. Jiang, Bioinspired hydrogel-polymer hybrids with a tough and antifatigue interface via one-step polymerization, ACS Appl. Mater. Interfaces 12 (45) (2020).

[141] M.P. Murphy, B. Aksak, M. Sitti, Gecko-inspired directional and controllable adhesion, Small 5 (2) (2009).

[142] L. Xi, L. Shi, X. Wan, B. Dai, M. Yang, Z. Gu, X. Shi, L. Jiang, S. Wang, A spider-silk-inspired wet adhesive with supercold tolerance, Adv. Mater. 33 (14) (2021).

[143] Y. Lee, S. Chun, D. Son, X. Hu, M. Schneider, M. Sitti, A tissue adhesion-controllable and biocompatible small-scale hydrogel adhesive robot, Adv. Mater. 34 (13) (2022).

[144] V.K. Venkiteswaran, S. Misra, Towards Gradient-Based Actuationof Magnetic Soft Robots Using a Six-Coil Electromagnetic System, IEEE, 2020.

[145] R. Bansil, B.S. Turner, The biology of mucus: composition, synthesis and organization, Adv. Drug Deliv. Rev. 124 (2018).

[146] M.F. Maitz, Applications of synthetic polymers in clinical medicine, Biosurf. Biotribol. 1 (3) (2015).

[147] Y. Wu, X. Dong, J.K. Kim, C. Wang, M. Sitti, Wireless soft millirobots for climbing three-dimensional surfaces in confined spaces, Sci. Adv. 8 (21) (2022).

[148] C. Wang, A. Mzyk, R. Schirhagl, S. Misra, V.K. Venkiteswaran, Biocompatible film-coating of magnetic soft robots for mucoadhesive locomotion, Adv. Mater. Technol. (2023) 2201813. https://onlinelibrary.wiley.com/doi/pdf/10.1002/admt.202201813.

[149] T.G. Leong, C.L. Randall, B.R. Benson, N. Bassik, G.M. Stern, D.H. Gracias, Tetherless thermobiochemically actuated microgrippers, Proc. Natl. Acad. Sci. 106 (3) (2009) 703–708.

[150] W.B. Liechty, D.R. Kryscio, B.V. Slaughter, N.A. Peppas, Polymers for drug delivery systems, Annu. Rev. Chem. Biomol. Eng. 1 (2010) 149–173.

[151] L. Ionov, Biomimetic hydrogel-based actuating systems, Adv. Funct. Mater. 23 (36) (2013) 4555–4570.

[152] W. Zhao, L. Liu, F. Zhang, J. Leng, Y. Liu, Shape memory polymers and their composites in biomedical applications, Mater. Sci. Eng. C 97 (2019) 864–883.

[153] B.Q.Y. Chan, Z.W.K. Low, S.J.W. Heng, S.Y. Chan, C. Owh, X.J. Loh, Recent advances in shape memory soft materials for biomedical applications, ACS Appl. Mater. Interfaces 8 (16) (2016) 10070–10087.

[154] Y. Xia, Y. He, F. Zhang, Y. Liu, J. Leng, A review of shape memory polymers and composites: mechanisms, materials, and applications, Adv. Mater. 33 (6) (2021) 2000713.

[155] M.S. Paolini, O.S. Fenton, C. Bhattacharya, J.L. Andresen, R. Langer, Polymers for extended-release administration, Biomed. Microdevices 21 (2) (2019) 1–24.

[156] J.C. Breger, C. Yoon, R. Xiao, H.R. Kwag, M.O. Wang, J.P. Fisher, T.D. Nguyen, D.H. Gracias, Self-folding thermo-magnetically responsive soft microgrippers, ACS Appl. Mater. Interfaces 7 (5) (2015) 3398–3405. PMID: 25594664.

[157] E. Gultepe, J.S. Randhawa, S. Kadam, S. Yamanaka, F.M. Selaru, E.J. Shin, A.N. Kalloo, D.H. Gracias, Biopsy with thermally-responsive untethered microtools, Adv. Mater. 25 (4) (2013) 514–519.

[158] S. Mishra, Applications of shape memory alloys: a review, J. Thin Films Coat. Sci. Technol. Applicat. 2 (2) (2015).

[159] S. Sánchez, W. Xi, A.A. Solovev, L. Soler, V. Magdanz, O.G. Schmidt, Tubular micro-nanorobots: smart design for bio-related applications, in: Small-Scale Robotics. From Nano-to-Millimeter-Sized Robotic Systems and Applications: First International Workshop at ICRA 2013, Karlsruhe, Germany, May 6, 2013, Revised and Extended Papers 1, Springer, 2014, pp. 16–27.

[160] S. Laurent, J.-L. Bridot, L.V. Elst, R.N. Muller, Magnetic iron oxide nanoparticles for biomedical applications, Future Med. Chem. 2 (3) (2010) 427–449.

[161] G. Kósa, P. Jakab, G. Székely, N. Hata, Mri driven magnetic microswimmers, Biomed. Microdevices 14 (2012) 165–178.

[162] C.M. Heunis, Z. Wang, G. de Vente, S. Misra, V.K. Venkiteswaran, A magnetic bio-inspired soft carrier as a temperature-controlled gastrointestinal drug delivery system, Macromol. Biosci. (2023) 2200559. https://onlinelibrary.wiley.com/doi/pdf/10.1002/mabi.202200559.

[163] F. Ongaro, S. Scheggi, C. Yoon, F.V. den Brink, S.H. Oh, D.H. Gracias, S. Misra, Autonomous planning and control of soft untethered grippers in unstructured environments, J. Micro-Bio Robot. 12 (1) (2017) 45–52.

[164] O. Erin, D. Antonelli, M.E. Tiryaki, M. Sitti, Towards 5-dof control of an untethered magnetic millirobot via mri gradient coils, in: Proceedings of the 2020 IEEE International Conference on Robotics and Automation (ICRA), 2020, pp. 6551–6557.

[165] T. Kensicher, J. Leclerc, D. Biediger, D.J. Shah, I. Seimenis, A.T. Becker, N.V. Tsekos, Towards MRI-guided and actuated tetherless milli-robots: preoperative planning and modeling of control, in: 2017 IEEE/RSJ International Conference on Intelligent Robots and Systems (IROS), 2017, pp. 6440–6447.

[166] H. Ceylan, I.C. Yasa, U. Kilic, W. Hu, M. Sitti, Translational prospects of untethered medical microrobots, Progr. Biomed. Eng. 1 (1) (2019) 012002.

[167] S. Scheggi, K.K.T. Chandrasekar, C. Yoon, B. Sawaryn, G. van de Steeg, D.H. Gracias, S. Misra, Magnetic motion control and planning of untethered soft grippers using ultrasound image feedback, in: Proceedings of the 2017 IEEE International Conference on Robotics and Automation (ICRA), 2017, pp. 6156–6161.

[168] I.S.M. Khalil, P. Ferreira, R. Eleutério, C.L. de Korte, S. Misra, Magnetic-based closed-loop control of paramagnetic microparticles using ultrasound feedback, in: Proceedings of the 2014 IEEE International Conference on Robotics and Automation (ICRA), 2014, pp. 3807–3812.

[169] M. Turan, Y. Almalioglu, H. Araujo, E. Konukoglu, M. Sitti, Deep EndoVO: a recurrent convolutional neural network (RCNN) based visual odometry approach for endoscopic capsule robots, Neurocomputing 275 (2018) 1861–1870.

[170] A.J.A. de Oliveira, J. Batista, S. Misra, V.K. Venkiteswaran, Ultrasound tracking and closed-loop control of a magnetically-actuated biomimetic soft robot, in: 2022 IEEE/RSJ International Conference on Intelligent Robots and Systems (IROS), 2022, pp. 3422–3428.